



HAL
open science

Decoding β -Cyclocitral-Mediated Retrograde Signaling Reveals the Role of a Detoxification Response in Plant Tolerance to Photooxidative Stress

Stefano d'Alessandro, Brigitte Ksas, Michel Havaux

► **To cite this version:**

Stefano d'Alessandro, Brigitte Ksas, Michel Havaux. Decoding β -Cyclocitral-Mediated Retrograde Signaling Reveals the Role of a Detoxification Response in Plant Tolerance to Photooxidative Stress. *The Plant cell*, 2018, 30 (10), pp.2495-2511. 10.1105/tpc.18.00578 . cea-01945901

HAL Id: cea-01945901

<https://cea.hal.science/cea-01945901>

Submitted on 8 Jan 2019

HAL is a multi-disciplinary open access archive for the deposit and dissemination of scientific research documents, whether they are published or not. The documents may come from teaching and research institutions in France or abroad, or from public or private research centers.

L'archive ouverte pluridisciplinaire **HAL**, est destinée au dépôt et à la diffusion de documents scientifiques de niveau recherche, publiés ou non, émanant des établissements d'enseignement et de recherche français ou étrangers, des laboratoires publics ou privés.

1 RESEARCH ARTICLE

2
3
4

5 **Decoding β -cyclocitral-mediated Retrograde Signaling Reveals the Role of a**
6 **Detoxification Response in Plant Tolerance to Photooxidative Stress**

7
8
9

10 **Stefano D'Alessandro, Brigitte Ksas and Michel Havaux***

11 Aix-Marseille Univ., CEA, CNRS, UMR 7265, BIAM, Laboratoire d'Ecophysiologie Moléculaire des Plantes,
12 CEA/Cadarache, F-13108 Saint-Paul-lez-Durance, France

13

14 **Corresponding Author:** Michel Havaux (michel.havaux@cea.fr)

15
16

17 **Short Title:** β -Cyclocitral induces a SCL14-dependent detoxification response

18
19
20

21 **One-sentence summary:** β -cyclocitral, generated in the chloroplast under high light stress, mitigates
22 photooxidative stress by recruiting the xenobiotic response involving SCL14, TGAI1, and ANAC102
23 transcription factors.

24
25
26

27 The author responsible for distribution of materials integral to the findings presented in this article in
28 accordance with the policy described in the Instructions for Authors (www.plantcell.org) is: Michel
29 Havaux (michel.havaux@cea.fr)."

30
31
32

33 **ABSTRACT**

34 When exposed to unfavorable environmental conditions, plants can absorb light energy in excess
35 of their photosynthetic capacities, with the surplus energy leading to the production of reactive
36 oxygen species and photooxidative stress. Subsequent lipid peroxidation generates toxic reactive
37 carbonyl species whose accumulation culminates in cell death. β -cyclocitral, an oxidized by-
38 product of β -carotene generated in the chloroplasts, mediates a protective retrograde response
39 that lowers the levels of toxic peroxides and carbonyls, limiting damage to intracellular
40 components. In this study, we elucidate the molecular mechanism induced by β -cyclocitral in
41 *Arabidopsis thaliana* and show that the xenobiotic detoxification response is involved in the
42 tolerance to excess light energy. The involvement of the xenobiotic response suggests a possible
43 origin for this pathway. Furthermore, we establish the hierarchical structure of this pathway that
44 is mediated by the β -cyclocitral-inducible GRAS protein SCL14 (SCARECROW LIKE 14) and involves
45 ANAC102 as a pivotal component upstream of other ANAC transcription factors and of many
46 enzymes of the xenobiotic detoxification response. Finally, the SCL14-dependent protective
47 mechanism is also involved in the low sensitivity of young leaf tissues to high light stress.

48

49 **Key words:** β -cyclocitral, xenobiotic response, stress response, excessive light, lipid peroxidation

50

51 **INTRODUCTION**

52

53 Plants often encounter light intensities that exceed their photosynthetic capacities, due to
54 unfavorable environmental conditions that prevent a good match between absorbed light energy
55 and carbon metabolism (Ort, 2001). The photosynthetic electron transport chain uses molecular
56 oxygen as an electron carrier, generating biologically damaging molecules such as reactive oxygen
57 species (ROS), peroxides and radicals (Asada, 2006; Apel and Hirt, 2004; Li et al., 2009). In
58 particular, triplet excited chlorophylls, whose lifetime increases under excess light conditions, can
59 transfer excitation energy directly to oxygen resulting in the formation of singlet oxygen (1O_2)
60 (Triantaphylidès and Havaux, 2009; Krieger-Liszkay et al., 2008). Besides its toxic effects, 1O_2 can
61 trigger a specific signaling cascade, leading to programmed cell death or to acclimation (Wagner

62 et al., 2004; Ramel et al., 2013a; Gadjev, 2006; Chan et al., 2016). Nevertheless, due to a high
63 reactivity and short lifetime (~ 100 ns in biological tissues), direct involvement of $^1\text{O}_2$ in retrograde
64 signaling is unlikely; rather, signaling may originate in the oxidation of preferential targets, which
65 then act as mediators.

66 Carotenoids are efficient $^1\text{O}_2$ physical quenchers (Frank and Cogdell, 1996) which are
67 sometimes oxidized by $^1\text{O}_2$ at the level of photosystem II, generating, among other products, the
68 retrograde signaling mediators β -cyclocitral (β -cc) and dihydroactinidiolide (Shumbe et al., 2017;
69 Ramel et al., 2012b; Shumbe et al., 2014; Havaux, 2014). β -cc is generated in the chloroplast and
70 its basal level (ca. 50 ng g^{-1} fresh leaf weight) triples during high light stress while
71 dihydroactinidiolide concentration (ca. 5 ng g^{-1}) increases almost tenfold, suggesting chronic
72 production of $^1\text{O}_2$ during photosynthesis and a dramatic increase under stress conditions (Ramel
73 et al., 2012b). Interestingly, treatment of plants with exogenous β -cc or dihydroactinidiolide
74 increases their internal leaf concentrations to levels comparable with the ones measured under
75 stress conditions (ca. 180 and 45 ng g^{-1} , respectively) and elicit a genetic response leading to
76 acclimation to high light stress (Ramel et al., 2012b; Shumbe et al., 2014).

77 A striking feature of the gene regulation induced by β -cc in Arabidopsis is the induction of
78 various detoxification mechanisms, among which the induction of several Glutathione-S-
79 transferases (GST) and UDP-glycosyltransferases (Ramel et al., 2012b) that also participate in
80 Phase II of the xenobiotic detoxifying process (Sandermann, 1992). In fact, in plants, ectopic
81 reactive chemicals are inactivated by a set of detoxifying enzymes that modify and eliminate these
82 compounds in three phases: modification, conjugation and compartmentalization (Riechers et al.,
83 2010; Sandermann, 1992). While the conjugation phase has been reported to be induced under
84 many different stresses, the modification phase has only been characterized more recently and
85 its involvement in physiological responses is still unclear (Riechers et al., 2010; Mueller et al.,
86 2008; Ramel et al., 2012c). In particular, in the modification phase, the GRAS protein SCARECROW
87 LIKE 14 (SCL14) and the Glutaredoxin GRX480/ROXY19 compete for binding with the TGA II
88 transcription factors and mediate the activation or the inhibition, respectively, of the
89 detoxification response (Huang et al., 2016; Fode et al., 2008; Köster et al., 2012; Ndamukong et
90 al., 2007).

91 In this work, we identify a SCL14-dependent xenobiotic detoxification response to a
92 physiological condition, rather than an artificial stimulus. Furthermore, we decode its role in the
93 β -cc-induced retrograde signaling that occurs under high light stress, and we show that SCL14-
94 dependent detoxification is necessary for the resilience of Arabidopsis plants to photooxidative
95 stress. In this work, we enrich our understanding of the SCL14-dependent pathway by showing
96 the hierarchical relationship between several players and make the link between the xenobiotic
97 detoxification pathway and its physiological role in detoxifying toxic reactive carbonyl species
98 (RCS). Finally, we show that SCL14 mediates part of the intrinsic resistance of young leaves to
99 excessive light.

100

101 RESULTS

102

103 β -cyclocitral elicits an excessive light-like response involving the TGA and MYC transcription 104 factors

105 The comparison of the genetic response of 5-week-old *Arabidopsis thaliana* plants treated with
106 β -cc (100 μ l β -cc for 4 h, <http://urgv.evry.inra.fr/CATdb>; Project: CEA10-03_Cyclocitral) with the
107 response of $^1\text{O}_2$ -overproducing *ch1* mutant plants exposed to excessive light (1200 μ mol photons
108 $\text{m}^{-2} \text{s}^{-1}$ at 10°C for 24h, Project: CEA10-02_Light) (Ramel et al., 2013b) revealed a 30% overlap of
109 the genes modified more than 1.5 fold in \log_2 values (Figure 1A). The overlap suggests the
110 existence of common mechanisms to cope with photooxidative damage, elicited by β -cc and
111 during enhanced production of $^1\text{O}_2$.

112 The regulatory regions of the 153 genes in the common cluster (-1000 to + 50 base pairs
113 from the starting codon) show an enrichment of the MYC (MYC2, 3 and 4) and of the TGA (class I
114 and II) transcription factor-binding sites (AthaMap gene analysis (Steffens, 2004)) (Figure 1B).
115 MYC transcription factors are activators of the jasmonic acid response, while TGA transcription
116 factors are well known players in the salicylic acid response and in detoxifying mechanisms (Chini
117 et al., 2007; Mueller et al., 2008; Kesarwani et al., 2007). Moreover, the interaction of SCL14 with
118 the TGA transcription factors induces the expression of a subset of the detoxification genes,
119 mainly belonging to the modification phase of the xenobiotic detoxification pathway (Fode et al.,

120 2008; Köster et al., 2012). Altogether, the MYC and TGA transcription factors mediate the
121 response to xenobiotics and their concerted action is required for the complete activation of the
122 response. In fact, as highlighted in the analysis of the expression of the phase-I enzyme
123 cytochrome P450 *CYP81D11* (Köster et al., 2012), only the activation of both the MYC and TGA
124 pathways leads to the maximum induction of the latter gene.

125

126 **β -cyclocitral and excessive light induce SCL14-regulated ANAC transcription factors**

127 Among the modified genes identified in the aforementioned transcriptomes, the expression
128 levels of the SCL14-regulated *ANAC002* and *ANAC032*, and of the related *ANAC081* and *ANAC102*
129 genes (Fode et al., 2008; Ratnakaran, 2014) have been further analyzed by reverse transcription
130 quantitative PCR (RT-qPCR) in control and β -cc-treated wild type (wt) plants and in plants after
131 excessive light stress (1500 $\mu\text{mol photons m}^{-2} \text{ s}^{-1}$ at 7°C for 24h). This analysis confirmed the
132 induction of the four *ANAC* genes by β -cc (respectively 20, 20, 13 and 50 times the control levels),
133 further pointing to *ANAC102* as the most induced ANAC transcription factor by the β -cc treatment
134 (Figure 1, C).

135 Furthermore, the stronger induction of *ANAC002*, *ANAC032* and *ANAC081* under
136 excessive light (respectively 50, 30 and 130 times the control values) suggests the coexistence of
137 several molecular signals able to induce this pathway generated by high light stress. The origin of
138 the pathway induced by xenobiotics is still unclear, and several mechanisms elicit the conjugation
139 phase of the xenobiotic response (Riechers et al., 2010). Among these, the response to oxylipins,
140 such as jasmonic acid, and lipid-derived reactive electrophilic compounds like 12-oxo-
141 phytodienoic acid (OPDA) and phytoprostanes (Riechers et al., 2010; Mueller and Berger, 2009),
142 with all these species being present in excessive light stress (Mano et al., 2005; Mano, 2012;
143 Farmer and Mueller, 2013). Conversely, here we highlight the activation of the modification phase
144 of the xenobiotic response under physiological conditions.

145

146 **β -cyclocitral induces a SCL14-regulated response**

147 β -cc enhances the expression of the four ANAC transcription factors involved in the SCL14-
148 dependent response to xenobiotics, and therefore we wanted to test the involvement of the TGA-

149 SCL14 regulation in the β -cc response. The TGA family of transcription factors and the
150 corresponding cis-element *as-1* are well-described transcriptional control mechanisms in plants
151 (Katagiri et al., 1989; Redman et al., 2002). The *as-1* element, from the CAMV 35S viral promoter,
152 and the *ocs* element, from the bacterial octopine synthase promoter, in the form of TGACG
153 sequences in the promoter, are mainly activated by the TGA II transcription factors, under auxin
154 and salicylic acid mediated stimuli (Lam and Lam, 1995). *As-1*-bound TGA transcription factors
155 recruit the GRAS protein SCL14 to the transcription site, activating several genes inducible by
156 xenobiotics, which contribute to the protection of plants (Mano, 2012; Turóczy et al., 2011; Mano
157 et al., 2005; Kotchoni et al., 2006; Fode et al., 2008).

158 To determine whether the SCL14-dependent xenobiotic detoxification pathway is
159 implicated in the genetic response induced by β -cc, we analyzed *ANAC002*, *032*, *081* and *102*
160 expression levels in the *tga II* and *scl14* mutant lines and in the *SCL14* overexpressing line
161 (OE:SCL14) by RT-qPCR after the β -cc treatment. These analyses showed that β -cc induction of
162 the ANAC transcription factors is weakened or impeded in the *tgaII* and *scl14* mutant lines (70 to
163 90% lower), while it is strengthened in the SCL14 overexpressing lines (200 to 800% higher)
164 (Figure 2).

165 In the response to salicylic acid, TGA II transcription factors can interact with NPR1 (Fan
166 and Dong, 2002; Després et al., 2000; Zhou et al., 2000). We tested an eventual competition
167 between NPR1 and SCL14 on the induction of the ANAC genes regulated by TGA 2, 5 and 6 by
168 analyzing *ANAC002*, *032*, *081* and *102* expression levels in the *npr1* mutant lines by RT-qPCR after
169 the β -cc treatment. The genetic response of the four SCL14-dependent ANAC transcription
170 factors, ANAC002, ANAC032, ANAC081 and ANAC102, to β -cc was similar in the *npr1-1* mutant
171 and in wt suggesting no competition between the two TGA regulating proteins under these
172 conditions (Supplemental Figure 1).

173 The participation of SCL14 in the response to exogenous artificial molecules is well known,
174 and many xenobiotics are able to induce the SCL14-dependent detoxification pathway (Riechers
175 et al., 2010; DeRidder et al., 2002; De Veylder et al., 1997; Taylor et al., 2013; Skipsey et al., 2011;
176 Fode et al., 2008). On the contrary, β -cc is an endogenous molecule showing a SCL14-dependent

177 response. This suggests that the SCL14-regulated response is more general than the detoxification
178 of xenobiotics and could play a role in the response to changes in natural environments.

179

180 **β -cyclocitral induces SCL14**

181 As the SCL14-dependent response was enhanced by the β -cc treatment, we analyzed the
182 expression level of *SCL14* itself. We confirm that *SCL14* is not expressed in the *scl14* mutant,
183 neither in control conditions nor in plants treated with β -cc (Figure 2). Then, we show that SCL14
184 is expressed 1.5 times more in the OE:SCL14 than in wt in control conditions, in line with the
185 protein levels previously described (Fode et al., 2008). Although being under the control of a 35S
186 constitutive promoter, *SCL14* transcript levels exhibited a relatively small increase in the OE:SCL14
187 line, suggesting the intervention of a post-transcriptional regulation. Finally, β -cc treatment
188 upregulated *SCL14* expression both in wt and in the OE:SCL14 lines (Figure 2). Remarkably, the
189 faint “overexpression” present in the OE:SCL14 was able to mediate a marked increase in the
190 response of ANAC genes to β -cc (200 to 800% higher in the OE:SCL14 than in the wt). Therefore,
191 the increase in *SCL14* gene expression observed in WT in response to β -cc (in the same range as
192 the SCL14 overexpressor in the absence of β -cc treatment), together with the concomitant
193 activation of the MYC pathway (Figure 1B), could explain the substantial effects of the
194 apocarotenoid on ANAC transcription factors (Figure 2) and on genes encoding detoxifying
195 enzymes (below, Figure 5) (Köster et al., 2012).

196

197 **SCL14 mediates plant resilience to excessive light**

198 SCL14 regulates the genetic response of plants treated with β -cc, and consequently we wondered
199 about the role of SCL14 under excessive light stress, which causes endogenous increases of β -cc
200 in a much more complex metabolic response. Therefore, we analyzed the behavior of the *scl14*
201 knockout mutant and the OE:SCL14 overexpressor under excessive light stress (1500 μmol
202 photons $\text{m}^{-2} \text{s}^{-1}$ at 7°C for 24h) following pre-treatment with β -cc or with water (100 μl for 4 h).
203 Lipid peroxidation was used as a marker of photooxidative damage and analyzed by image
204 quantification of plant autoluminescence, derived from the spontaneous decomposition of lipid
205 peroxides (Birtic et al., 2011), and by HPLC-UV quantification of HOTEs (hydroxy octadecatrienoic

206 acid isomers) derived from the oxidation of linolenic acid (Birtic et al., 2011; Montillet et al., 2004).
207 *sc/14* plants showed stronger leaf bleaching after 24-h exposure to stress conditions as compared
208 to wt plants, as well as more intense lipid-peroxidation-related luminescence (Figure 3, A). By
209 contrast, OE:SCL14 plants showed almost no detrimental effects due to the stress conditions. The
210 sensitive and resistant behaviors of *sc/14* and OE:SCL14 lines were confirmed by the quantification
211 of HOTE in leaf samples of the stressed plants, showing 1.5-time higher HOTE levels in the mutant
212 line and five times lower HOTE levels in the overexpressing line compared to wt (Figure 3, B).

213 SCL14 has been shown to interact with TGA 2, 5 and 6 transcription factors and to co-
214 regulate at least a subset of the genes presenting the TGA binding *as-1* motif in their promoter
215 (Fode et al., 2008). We consequently evaluated the role of the TGA 2, 5 and 6 transcription factors
216 in the response to excessive light by exposing the *tga //* triple mutant line to stress conditions
217 following pre-treatment with β -cc or with water. *tga //* plants showed stronger leaf bleaching after
218 24-h exposure to stress conditions as compared to wt plants, as well as more intense lipid-
219 peroxidation-related luminescence (Figure 4, A). The sensitive behaviors of the *tga //* line was
220 confirmed by the quantification of HOTE in leaf samples of the stressed plants, showing 1.5-time
221 higher HOTE levels in the mutant line compared to wt (Figure 4, B).

222

223 ***sc/14* mutant lines are not able to acquire β -cc-induced resistance to excessive light**

224 A 4-h β -cc pre-treatment of wt plants is sufficient to induce a genetic response leading to
225 acclimation to excessive light stress (Ramel et al., 2012b; Shumbe et al., 2017). The acclimated
226 status is indicated by a lower accumulation of lipid peroxides under excessive light stress (< 50%
227 compared to untreated plants), revealed by plant autoluminescence and HPLC-UV HOTE
228 quantification (Ramel et al., 2012b). The treatment of plants with β -cc, sufficient to protect wt
229 plants from photooxidative stress (Figure 3A and B), was ineffective on *sc/14* mutant lines. β -cc-
230 treated *sc/14* plants showed comparable leaf bleaching and autoluminescence to untreated
231 samples (Figure 3, A). In addition, the quantification of HOTE confirmed the inability of *sc/14*
232 mutant plants to acquire the β -cc-induced acclimation to excessive light (Figure 3, B). The lack of
233 β -cc-induced protection in the *sc/14* mutant line highlights SCL14 as central actor in the β -cc
234 signaling network leading to acclimation. These results demonstrate that SCL14 is not only

235 necessary for the proper genetic response to β -cc and excessive light, but that xenobiotic
236 detoxification is necessary both for light-induced acclimation to photooxidative stress and for β -
237 cc-induced acclimation.

238 Similarly as in *sc14*, the treatment of *tga II* plants with β -cc was ineffective. In fact, β -cc-
239 treated *tga II* plants showed comparable leaf bleaching and autoluminescence to untreated
240 samples (Figure 4, A). In addition, the quantification of HOTE confirmed the inability of *tga II*
241 mutant plants to acquire the β -cc-induced acclimation to excessive light (Figure 4, B). Results of
242 Figure 4 show that the *tgaII* mutant phenocopies the *sc14* mutant at the whole plant level (Figure
243 3).

244

245 **β -cyclocitral induces a SCL14-dependent xenobiotic detoxification response**

246 The response to β -cc is, at least in part, dependent on SCL14, but the SCL14-dependent xenobiotic
247 response is an integrated network involving many molecular targets. Among these, four ANAC
248 transcription factors (ANAC 2, 32, 81, 102) and families of modifying enzymes, like cytochrome
249 P450s, short chain dehydrogenases/reductases (SDR), monooxygenases, 2-alkenal reductases
250 (AER), aldo-keto reductases (AKR) and aldehyde dehydrogenases (ALDH), take part in the
251 modification phase of the xenobiotic response (Fode et al., 2008). The analysis of the
252 transcriptome of β -cc-treated plants suggests that many of these genes are also induced by β -cc,
253 and we further verified by RT-qPCR the expression of a selection of genes: *ChIADR*
254 (*CHLOROPLASTIC ALDEHYDE REDUCTASE*, AT3G04000), *SDR1* (*SHORT-CHAIN*
255 *DEHYDROGENASE/REDUCTASE 1*, AT4G13180), *AER* (*ALKENAL REDUCTASE*, AT5G16970), *AKR4C9*
256 (*CHLOROPLASTIC ALDO-KETO REDUCTASE*, ChIAKR, AT2G37770), *GRX480/ROXY19* (AT1G28480)
257 and a gene of unknown function but strongly induced by β -cc (AT5G61820). These analyses
258 showed that induction of the selected genes by β -cc is weakened or impeded in the *tgaII* and
259 *sc14* mutant lines (70 to 99% lower), while it is strengthened in the SCL14 overexpressing lines
260 (150 to 1000% higher) (Figure 5). Therefore, we can confidently conclude that β -cc is able to
261 induce a xenobiotic-like response (Riechers et al., 2010; Kreuz et al., 1996; Sandermann, 1992).

262 Furthermore, these families of enzymes are of particular interest when we consider lipid
263 peroxidation occurring under excessive light stress, especially in the chloroplast. In this stress,

264 lipid peroxides mainly derive from the linoleic (18:2), linolenic (18:3), and roghanic (16:3)
265 polyunsaturated fatty acids (PUFAs) (Montillet et al., 2013). These primary hydroperoxy or
266 hydroxy fatty acids can generate aldehydes, oxo-acids, epoxydes, and cyclized compounds such
267 as jasmonates or phytoprostanes (Montillet et al., 2013; Mano et al., 2005). Several of these
268 compounds are reactive carbonyls (Mano, 2012) that can specifically be anabolized by the SDR,
269 AER, AKR and ALDH enzyme families, exactly the same as those induced by the xenobiotic
270 response (Mano et al., 2005; Yamauchi et al., 2011; Mano, 2012). Furthermore, chloroplasts are
271 the main sites of lipid peroxidation under excessive light stress, and at least two of the enzymes
272 induced by β -cc, the chloroplastic aldehyde reductase (ChIADR) and the chloroplastic aldo-keto
273 reductase (ChIAKR), can detoxify RCS directly at the primary location of production, as they are
274 expressed in the stroma (Yamauchi et al., 2011).

275

276 ***anac102* mutant lines are sensitive to excessive light and unresponsive to β -cc**

277 *ANAC102* was the most induced SCL14-dependent ANAC transcription factor by the treatment
278 with β -cc. Therefore, we analyzed *anac102* knockout mutant plants, pre-treated with β -cc or with
279 water, under excessive light stress ($1500 \mu\text{mol photons m}^{-2} \text{s}^{-1}$ at 7°C for 24h). 5-week-old *anac102*
280 plants showed stronger leaf bleaching after 24-h exposure to stress conditions as compared to wt
281 plants, as well as enhanced lipid-peroxide-dependent autoluminescence (Figure 6A). The
282 photosensitive behavior of *anac102* was confirmed by the quantification of HOTEs in leaf samples
283 of the stressed plants, which showed three times higher HOTE levels in the mutant line compared
284 to wt (Figure 6B). Furthermore, β -cc-treated *anac102* plants showed comparable leaf bleaching
285 and autoluminescence as untreated samples (Figure 6A), indicating that β -cc signaling was
286 incomplete in this mutant. In addition, HOTE quantification confirmed the inability of *anac102*
287 mutant plants to acquire the β -cc-induced acclimation to excessive light (Figure 2B). The lack of
288 β -cc-induced protection in the *anac102* mutant line implies that ANAC102 participates in the β -
289 cc retrograde signaling downstream of SCL14.

290

291 **β -cyclocitral-induced SCL14-dependent detoxification response is blocked in *anac102***

292 We verified by RT-qPCR the expression of SCL14-dependent genes, *ChiADR*, *SDR1*, *AER*, *AKR4C9*
293 (*ChiAKR*), *GRX480/ROXY19* and *AT5G61820*, in wt and *anac102* mutant lines. These analyses
294 showed that β -cc induction of the selected genes is weakened or impeded in the *anac102* mutant
295 (90 to 99% lower) (Figure 7). These results place ANAC102 downstream of SCL14, as previously
296 shown (Fode et al., 2008), but upstream of the analyzed detoxifying enzymes.

297

298 **ANAC102 is upstream of ANAC002, ANAC032 and ANAC081**

299 To better elucidate the molecular pathway downstream of SCL14 in the response to β -cc, we
300 analyzed the expression levels of *ANAC002*, *ANAC032* and *ANAC081* in wt and in the *anac102*
301 mutant line. The analyses showed that β -cc induction of the three SCL14-regulated ANAC
302 transcription factors was completely blocked in the *anac102* mutant line (Figure 8). This finding
303 reveals transcriptional control of *ANAC002*, *ANAC032* and *ANAC081* transcription factors by
304 ANAC102 in the SCL14-dependent pathway. By these analyses, we have shown not only that
305 ANAC102 controls the induction of the detoxification enzymes, previously reported at the same
306 level of ANAC102 (Fode et al., 2008), but also that ANAC transcription factors follow a hierarchical
307 order in β -cc retrograde signaling.

308

309 **SCL14-dependent detoxification pathway is independent of MBS1**

310 β -cyclocitral elicits the SCL14-dependent xenobiotic response pathway to mediate the
311 phototolerance to excessive light. However, it was recently demonstrated that β -cc retrograde
312 signaling depends on the MBS1 protein (Shumbe et al., 2017). We then wondered whether the
313 two pathways are interdependent or operate in parallel. By analyzing the genetic response of
314 *ANAC032*, *ANAC102*, *ChiADR*, *SDR1*, *AER*, *AKR4C9* (*ChiAKR*) and *AT5G61820* to β -cc in the *mbs1*
315 mutant line (Figure 9), we found that all those marker genes of detoxification were equally
316 induced, or had a limited induction, in the mutant line compared to wt. Based on the normal
317 induction of the detoxification response in the *mbs1* mutant, we must hypothesize the
318 coexistence of at least two mechanisms downstream of β -cyclocitral: the MBS1-independent
319 detoxification response controlled by SCL14 and a pathway controlled by MBS1. Nevertheless,

320 under the rather severe light stress conditions used here (sudden transfer of plants from low light
321 to high light), both pathways appear to be required for β -cc-induced phototolerance.

322

323 **ANAC102 is particularly induced in young leaves**

324 We generated stable Arabidopsis transgenic lines carrying the full *ANAC102* (AT5G63790) gene (-
325 2041 +1124), including the putative 5' regulatory region and both introns and exons, coding for
326 the ANAC102 protein fused to the β -glucuronidase reporter. By histochemical assay, we show
327 that the ANAC102 reporter is present at low levels under physiological conditions (Figure 10,
328 Supplemental Figure 1), being detectable only in the conductive tissues of young leaves. On the
329 contrary, after the treatment with β -cc, the reporter strongly accumulated in the full limb of
330 young leaves as well as in the conductive tissues of mature leaves (Figure 10). We further verified
331 that the strong accumulation of ANAC102 in the β -cc-treated samples is due to an upregulation
332 of gene expression rather than a stabilization of the ANAC102- β -glucuronidase fusion protein.
333 Samples treated with the protein synthesis inhibitor cycloheximide did not show the
334 accumulation of the reporter (Supplemental Figure 2). In the light of the positive effect of
335 ANAC102 and SCL14 on the resilience to excessive light, the higher accumulation of ANAC102 in
336 young leaves suggests that the younger leaf tissues could be more resistant to this stress than the
337 old, mature tissues.

338

339 **Young leaves are more resistant to excessive light than mature leaves, and this difference is** 340 **dependent on SCL14**

341 As shown in Figure 3A and Figure 6A, young leaves in the center of the rosette do not show lipid-
342 peroxide-derived luminescence after high light stress, suggesting a high tolerance to
343 photooxidation. By using whole plants, resistance of younger tissues to excessive light could
344 depend both on biological factors like systemic acquired acclimation (SAA) (Rossel et al., 2007;
345 Carmody et al., 2016) and on technical factors like the heterogeneity of irradiance and leaf
346 temperature. To determine whether young leaves are intrinsically resistant to excessive light, we
347 cut young and mature leaves from several plants and placed them on a flat surface covered with
348 water, where irradiance and temperature during the stress are more homogeneous (1100 μ mol

349 photons $\text{m}^{-2} \text{s}^{-1}$ at 4°C for 16h). Furthermore, the cut-leaf system excludes the eventual
350 participation of the systemic and long-distance signaling to the high-light tolerance. By this
351 analysis, under more controlled conditions, we feel confident to confirm the higher resilience of
352 young leaves to excessive light compared to mature leaves by an organ autonomous mechanism.
353 In fact, not only autoluminescence after the stress was much lower in young leaves than in mature
354 leaves (Figure 11, A), but also the quantification of HOTE confirmed this difference (75% less HOTE
355 in young leaves) (Figure 11, C), and Fv/Fm was higher in young leaves, indicating lower
356 photoinhibition of the photosynthetic apparatus (Figure 11, B).

357 Leaves can acclimate to excessive light through molecular, anatomical and physiological
358 changes (Kouřil et al., 2013; Oguchi et al., 2003). In particular, younger leaves can better resist to
359 photoinhibition than older leaves due to a higher plasticity allowing a faster redesign of their
360 anatomy and photosynthetic apparatus, optimizing them to the new light conditions (Bielczynski
361 et al., 2017; Sims and Pearcy, 1992). Furthermore, many pathways can increase the
362 photoprotective capacity of younger leaves such as a higher capacity to accumulate ascorbate
363 peroxidase (APX) and superoxidase dismutase (SOD) (Moustaka et al., 2015). Both enzymes are
364 part of the ROS scavenging system, allowing lower oxidative damage upstream of lipid
365 peroxidation.

366 To discern the involvement of SCL14 in the response of young leaves to high light, we
367 tested leaves cut from 5-week-old *sc14* mutant plants or SCL14 overexpressing lines. The
368 excessive light treatment induced lower photooxidative stress in OE:SCL14 leaves compared to
369 wt, as shown by a lower autoluminescence intensity. On the contrary, *sc14* leaves showed much
370 stronger luminescence both in mature and young leaves (Figure 11, A). These results were also
371 confirmed by the HPLC-UV quantification of HOTE, showing higher HOTE levels in *sc14* mature
372 and young leaves compared to wt mature and young leaves (Figure 11, C). In addition, young
373 leaves of the *sc14* mutant line showed a weaker intrinsic resistance to high light compared to
374 young tissues of wt. While in wt we found a strong decrease in lipid peroxidation (75% less HOTE)
375 in young leaves relative to mature leaves, we found only a partial protection (40% less HOTE) of
376 young tissues compared to mature ones in the *sc14* mutant (Figure 11, C). Furthermore, HOTE
377 levels found in mature leaves of OE:SCL14 lines were much lower than in wt leaves (25% of HOTE

378 levels present in wt mature leaves) and comparable to the ones found in young wt leaves. In
379 addition, reduced photodamage of the photosynthetic apparatus were observed in OE:SCL14
380 lines as shown by the high Fv/Fm chlorophyll fluorescence ratio values (Figure 11, B), while
381 greater photodamage was observed in *sc14* mutant leaves. Considering these results, we can
382 conclude that the SCL14-dependent response participates in the resilience of young leaves to
383 excessive light, in parallel to their higher photoprotective capacities.

384

385 **SCL14-dependent detoxification pathway acts on toxic RCS rather than on ROS accumulation**

386

387 In Figure 3 and 11, we show higher lipid peroxidation in the *sc14* mutant line compared to wt,
388 and a marked resistance of the OE:SCL14 line. The enzymes, whose transcriptional levels are
389 controlled by SCL14, take part in the modification phase of the xenobiotic detoxification response
390 (Sandermann, 1992; Fode et al., 2008). These enzymes are able to detoxify toxic RCS, mainly
391 aldehydes, to less reactive carboxylates or alcohols (Mano et al., 2005; Mano, 2012; Yamauchi et
392 al., 2011). RCS are not merely markers of oxidative stress, but rather active factors that can
393 deplete glutathione pools and then exacerbate stress effects (Mano, 2012). We tested this idea
394 in our stress conditions by pre-treating wt plants with 1 mM 4-hydroxy-nonenal (HNE), a well-
395 known RCS detoxified by AER (Mano, 2012; Mano et al., 2005). As shown in Figure 12A, a 4-h
396 treatment with HNE worsened plant fitness against excessive light stress and amplified oxidative
397 damage. In fact, treated plants showed higher autoluminescence and increased HOTE level after
398 high light stress compared to control plants (Figure 12A). We can therefore confirm that the
399 higher peroxidation levels found in the *sc14* mutant line can be due to inefficient RCS scavenging
400 that leads to amplified oxidative damage. On the contrary, the lower peroxidation found in the
401 OE:SCL14 lines is compatible with an enhanced detoxification response, thus with reduced RCS
402 levels and consequent oxidative damage. For the HNE treatment, for example, the *AER* gene is
403 induced 5-times more in the OE:SCL14 line than in wt by the β -cc treatment, while it is induced
404 4-times less in the *sc14* mutant line than in wt (Figure 5). In addition, we also analyzed ROS
405 accumulation in those mutant or transgenic lines by means of fluorescent dyes. OE:SCL14, wt and
406 *sc14* plants were put in stress conditions for 4 h and then infiltrated with the $^1\text{O}_2$ specific probe

407 SOSG (Singlet Oxygen Sensor Green) or with the general ROS probe H₂DCFDA, mainly responsive
408 to H₂O₂. The quantification of the fluorescence emitted by the ROS-activated probes, showed no
409 differences in ROS accumulation between the three genotypes (Figure 12C). Altogether, these
410 results suggest that the sensitivity of *sc/14* line and the tolerance of the OE:SCL14 lines to
411 excessive light are likely due to a different accumulation of RCS rather than differential ROS
412 accumulations.

413

414 **DISCUSSION**

415

416 For more than 25 years, it was known that plants are able to detoxify xenobiotic compounds
417 explaining, for example, different sensitivities to herbicides (Riechers et al., 2010; Kreuz et al.,
418 1996; Sandermann, 1992). Artificial molecules that enter the cells can elicit a detoxification
419 process that inactivates them by a three-phase mechanism. First, hydroxylases, reductases (i.e.
420 AER, AKRs and SDRs), cytochrome P450 monooxygenases or peroxidases introduce or modify
421 reactive side groups. In the second phase, these modified exogenous compounds are conjugated
422 to sugar moieties or glutathione by either glycosyl transferases or glutathione-S-transferases.
423 Finally, the conjugates are transported to the vacuole or to the apoplast (Sandermann, 1992). The
424 exact origin of the pathway elicited by xenobiotics is still unclear but several mechanisms can
425 participate in the response (Riechers et al., 2010). Among these, xenobiotics elicit a genetic
426 modification partially overlapping the response to oxylipins, such as jasmonic acid, or reactive
427 electrophilic lipid-derived compounds, like OPDA and phytoprostanes (Riechers et al., 2010;
428 Mueller and Berger, 2009).

429 The concentration of oxylipins, carbonyls and RCS, generated by enzymatic activities and
430 by ROS-dependent oxidation, increases under many stresses (Mano, 2012; Farmer and Mueller,
431 2013; Roach et al., 2017). In fact, ROS, lipid peroxides and RCS, corresponding to the α,β -
432 unsaturated aldehydes and ketones derived from lipid hydroperoxides, are critical cell-damaging
433 agents in plants under environmental stresses, which can lead to cell death (Mano, 2012). These
434 compounds characterize the oxidative response and they can be specifically inactivated by
435 families of enzymes of the detoxification pathway, such as AER, AKRs, SDRs, ALDHs (Mano, 2012).

436 The beneficial role of the latter enzymes for plant tolerance to environmental constraints has
437 been reported in several plant species (Mano, 2012; Turoczy et al., 2011; Mano et al., 2005;
438 Kotchoni et al., 2005; Stiti et al., 2011)

439 The β -carotene oxidation by-product β -cc, generated under photooxidative stress, is the
440 first identified non-artificial compound that can induce the SCL14-dependent xenobiotic
441 response, exploiting this pathway to confer resistance to excessive light. Furthermore, we show
442 that this response is independent of MBS1 signaling but equally necessary for coping with high
443 light stress and for the β -cc-induced resistance to high light. We identified for the first time the
444 SCL14-dependent-xenobiotics detoxification in response to a physiological condition, rather than
445 an artificial stimulus. In fact, plants lacking the TGAII-regulative factor SCL14, or the TGA2,5 and
446 6 transcription factors themselves (Figure 4), became sensitive to photooxidative stress. We
447 propose that the enhanced cell death and lipid peroxide accumulation found in these lines, is due
448 to a stunted induction of the detoxification response downstream of SCL14 and ANAC102. In fact,
449 high RCS levels, obtained by a pretreatment with 4-hydroxy-nonenal, made the plant more
450 sensitive to high light conditions. On the contrary, the overexpression of *SCL14* that permits a
451 stronger induction of the detoxification response was sufficient to confer increased resistance to
452 photooxidative stress. As under excessive light and considering that plants suffer excessive light
453 on a daily basis (Ort, 2001), it would be worth testing the overexpression of this regulative factor
454 under other stresses and in other plant species, to verify the possible impact of enhancing the
455 detoxification response on field yields, like previously described for single enzymes downstream
456 of SCL14 (Mano et al., 2005; Mano, 2012; Turóczy et al., 2011; Kotchoni et al., 2006; Stiti et al.,
457 2011).

458 Finally, we can state that the SCL14-dependent-xenobiotic response occurs during
459 photooxidative stress and that it participates in the β -cc-induced resistance to excessive light and
460 to the intrinsic resistance of young tissues to this stress. Therefore, we propose a mechanism in
461 which photooxidation under excessive light generates toxic RCS metabolites and increases β -cc
462 concentration. β -cc enhances SCL14 expression, likely increasing the number of interactions
463 between SCL14 and the *as1*-bound TGA transcription factors that, together with the activation of
464 the MYC-dependent signaling pathway (Figure 1), induces strong activation of the xenobiotic

465 detoxification response (Figure 13) (Köster et al., 2012). In fact, the concerted action of the TGA
466 and the MYC transcription factors is required for the complete activation of the detoxification
467 response (Köster et al., 2012). Furthermore, the limited induction of SCL14 by β -cc, similar to the
468 overexpression levels found in the OE:SCL14 line, could explain why we detected no competition
469 between SCL14 and NPR1, one of the many interacting protein partners of the TGAII transcription
470 factors (Fan and Dong, 2002; Després et al., 2000; Zhou et al., 2000). In fact, the genetic response
471 of the four SCL14-dependent ANAC transcription factors, ANAC002, ANAC032, ANAC081 and
472 ANAC102, to β -cc was similar in the *npr1-1* mutant and in wt (Supplementary Figure 2)

473 In this work, we enrich the SCL14-dependent pathway by showing the hierarchical
474 relationship between the several players and make the link between the response to xenobiotics
475 and its physiological role in detoxifying toxic reactive carbonyl species (RCS), which have a
476 negative impact under stress conditions. More specifically, we show that among all the elements
477 regulated by SCL14, ANAC102 is a master regulator of the downstream response. Accordingly,
478 ANAC002, ANAC032 and ANAC081 were unresponsive to β -cc in the *anac102* mutant line (Figure
479 8).

480 Under excessive light, SCL14, TGA II and likely MYC transcription factors mediate the
481 induction of ANAC102. This transcription factor was shown to be indispensable for coping with
482 high light and to mediate the induction of ANAC002, ANAC032 and ANAC081 and, consequently,
483 of the downstream enzymes (Ratnakaran, 2014). Finally, the strong induction of the AER, AKR,
484 ALDH and SDR enzymes and of the glucosyl and glutathione transferases (Ramel et al., 2012b)
485 assures the elimination of RCS produced under stress conditions. RCS are toxic for the cell and
486 their accumulation leads to a reinforced accumulation of lipid peroxides under excessive light
487 (Figure 12) (Mano, 2012). The activation of this detoxification mechanism precludes cell death
488 owing to lower accumulation of toxic compounds and depicts a novel process by which β -cc
489 enhances plant performance under photooxidative stress (Figure 13). It is likely that the SCL14-
490 dependent pathway of Figure 13 is part of a more complex mechanism of phototolerance, which
491 could involve regulation of phytohormones such as jasmonic acid. Indeed, acclimation of the $^1\text{O}_2$ -
492 overproducing *ch1* Arabidopsis mutant is associated with a block of the biosynthesis of this

493 phytohormone in high light (Ramel et al., 2013b). Further studies will have to clarify the links
494 between the β -cc-induced detoxification pathway shown here and hormonal regulations.

495 Chloroplasts are the main sites of lipid peroxidation under excessive light stress, and at
496 least two of the enzymes induced by β -cc, the stroma-localized chloroplastic aldehyde reductase
497 (ChIADR) and the chloroplastic aldo-keto reductase (ChIAKR), can detoxify RCS directly at the
498 primary location of production. The perfect correspondence of the toxic metabolites produced
499 under oxidative stress with the target of the enzymatic families that compose the xenobiotic
500 response let us hypothesize a possible explanation for the origin of this pathway. In other words,
501 the exceptional diversity of reactive damaging molecules generated under photooxidative stress
502 could have led to the evolution of a general mechanism of detoxification that mediates the
503 inactivation of several reactive and potentially toxic compounds (Huang et al., 2016).

504 In this work, we further deciphered the intrinsic resistance of young tissues to excessive
505 light. Younger leaves can better resist photoinhibition than older leaves due to a higher plasticity
506 (Bielczynski et al., 2017; Sims and Pearcy, 1992) and to higher capacity to accumulate ascorbate
507 peroxidase (APX) and superoxidase dismutase (SOD) (Moustaka et al., 2015). In addition, high
508 light triggers both autonomous signals required for direct high light and ROS perception and non-
509 autonomous distal systemic acquired acclimation (SAA) (Carmody et al., 2016; Rossel et al., 2007).
510 Altogether, these mechanisms may participate in the tolerance to photooxidative stress in young
511 leaves under our stress conditions. In fact, we were unable to observe photooxidation in the
512 young leaves of whole plants (Figure 3, 6 and 12) and we had to increase stress conditions, by
513 prolonging the stress to 48h, to observe a limited peroxidation and photoinhibition in wt young
514 leaves (Supplementary Figure 3). Wt young leaves are resistant to high light both when whole
515 plants or cut leaves were put under stress conditions, suggesting autonomous mechanisms are
516 prevalent in the tolerance. On the other hand, young *sc14* leaves were drastically more sensitive
517 to high light than wt in the detached leaves experiments, while only limitedly more sensitive when
518 we analyzed whole plants (Supplementary Figure 3). This suggests an additional role for the
519 systemic acquired acclimation upstream of SCL14. In fact, when systemic signaling is excluded,
520 SCL14 is pivotal for reducing peroxidation, while other mechanisms are induced in young leaves

521 in a systemic way, that could limit RCS formation by reducing ROS concentrations (Carmody et al.,
522 2016; Matsuo et al., 2015).

523 To sum up, we propose a mechanism elicited by β -cc to achieve plant tolerance to high
524 light, in parallel with the previously described MBS1-mediated protection against singlet oxygen.
525 For the first time, the SCL14-dependent detoxification is linked to a physiological process rather
526 than to the resistance to artificial or synthetic xenobiotics. The induction of the many enzymes
527 belonging to the first phase of the detoxification can now be correlated with the increase in the
528 concentration of their substrates, namely oxidized lipids (e.g. HOTES) and derived metabolites.
529 Finally, we highlight a more complete and integrated view on the processes happening
530 downstream of photooxidation, which are schematized in Figure 13.

531

532 **METHODS**

533

534 **Plant growth and stress treatment**

535 Wild type (wt, ecotype *Col 0*) and *anac102* (SALK_030702C) were obtained from the Nottingham
536 Arabidopsis Stock Centre (Arabidopsis.info) (Christianson et al., 2009), *sc14*, the triple mutant
537 *tga II* (*tga 2x5x6*) and the SCL14-overexpressing *Arabidopsis thaliana* lines were kindly provided
538 by the Christiane Gatz laboratory (Göttingen, Germany) (Fode et al., 2008). The *npr1* mutant line
539 was kindly provided by Gerit Bethke of the Glazebrook lab (St. Paul, Minnesota). All the lines were
540 grown for 5 weeks in short-day conditions (8h/16h, day/night) under a moderate photon flux
541 density (PFD) of $\sim 150 \mu\text{mol photons m}^{-2} \text{ s}^{-1}$ provided by HQI metal halide bulbs (Osram),
542 controlled temperature (22 °C/18 °C, day/night) and a relative air humidity of 65 %.
543 Photooxidative stress was applied by subjecting at least 3 plants of wt, *anac102*, *sc14*, *tga II*, *npr1*
544 and OE:SCL14 lines per experiment, to $1500 \mu\text{mol m}^{-2} \text{ s}^{-1}$ PFD, 7 °C/18 °C temperature day/night
545 respectively, and 380 ppm CO₂ in a growth chamber (Ramel et al., 2012b; Havaux, 2014).
546 Alternatively, for the photooxidative stress on detached leaves, mature and young leaves were
547 cut from 5-week old plants of the different lines and placed on a flat and wet surface. Leaf age
548 was defined by leaf position (mature: leaves 5 – 11, young: leaves > 14) (Mousavi et al., 2013).
549 Stress conditions were imposed by placing the leaves in a cold chamber (6 °C) under a PFD of 1100

550 $\mu\text{mol photons m}^{-2} \text{s}^{-1}$ for 16 hours. β -cyclocitral (β -cc) treatment was performed by placing plants
551 in a transparent airtight plexiglass box, and by applying defined volumes (50 or 100 μl) of pure β -
552 cc on cotton balls in the plexiglass boxes (Ramel et al., 2012b; Shumbe et al., 2017, 2014). As a
553 control, β -cc was replaced with H_2O . The plexiglass boxes were thoroughly sealed and placed in
554 a growth chamber under controlled conditions of light and temperature ($50 \mu\text{mol photons m}^{-2} \text{s}^{-1}$
555 1 and 22°C) for 4 h. β -cc was obtained from Sigma-Aldrich.

556 The treatment with 4-HNE was performed by spraying plants with 1 mM 4-HNE in water
557 and putting the plant in sealed plexiglass boxes for 4h. As a control, 4-HNE was replaced with
558 water. Then high light stress conditions were imposed, as described above.

559 The translational reporter lines ANAC102:ANAC102-GUS were obtained by cloning the full
560 AT5G63790 gene (-2041 +1124), including the putative 5' regulative region and both introns and
561 exons, in frame to the uidA gene in the pBGWFS7 gateway entry vector (Karimi et al., 2002) (Table
562 S1). The vector was transformed in Agrobacterium C58C1 strain and wt plants were transformed
563 by floral dip.

564

565 **Quantification of lipid peroxidation and imaging**

566 Lipids were extracted from 0.3 to 0.5 g of leaves, deriving from a pool of 3 plants for each
567 condition, then frozen in liquid nitrogen. The leaves were ground in an equivolume
568 methanol/chloroform solution containing 5mM Triphenylphosphine (PO_3) and 1 mM 2,6-tert-
569 butyl-p-cresol (BHT) (5 ml g^{-1} fresh weight) and 1M citric acid (2.5 ml g^{-1} fresh weight), using an
570 Ultra-Turrax blender. 15-HEDE was added as an internal standard to a final concentration 100
571 nmol g^{-1} fresh weight and mixed properly. After centrifugation at 700 rpm and 4°C for 5 min, the
572 lower organic phase was carefully taken out with the help of a glass syringe and transferred into
573 a 15 ml glass tube. The syringe was rinsed with approximately 2.5 ml chloroform and emptied in
574 the tube containing the upper organic phase. The process was repeated, and the lower layer was
575 again collected and pooled with the first fraction. The solvent was evaporated under N_2 gas, at
576 40°C . The residues were recovered by 1.25 ml absolute ethanol and 1.25 ml of 3.5 N NaOH and
577 hydrolyzed at 80°C for 30 minutes. The ethanol was evaporated under N_2 gas at 40°C for ~ 10
578 minutes. After cooling to room temperature, pH was adjusted to 4 - 5 by adding 2.1 ml 1M citric

579 acid. Hydroxy fatty acids were extracted with hexane/ether 50/50 (v/v). The organic phase of
580 three samples for each condition was analyzed by straight phase HPLC-UV, as previously
581 described (Montillet et al., 2004). ROS-induced and LOX-mediated hydroxy octadecatrienoic acid
582 (HOTE) isomers (9-, 12-, 13- and 16-HOTE derived from the oxidation of the main fatty acid,
583 linolenic acid) were quantified based on the 15-HEDE internal standard (Montillet et al., 2004).
584 Lipid peroxidation was also visualized in whole plants by autoluminescence imaging. Stressed
585 plants were dark adapted for 2 h, and the luminescence emitted from the spontaneous
586 decomposition of lipid peroxides was captured by a highly sensitive liquid N₂- cooled charge-
587 coupled device (CCD) camera, as previously described (Birtic et al., 2011). One exemplificative
588 plant was analyzed for each condition, and experiments were repeated at least twice. The images
589 were treated using Image J software (NIH, USA)

590

591 **PSII photochemical activity**

592 Chlorophyll fluorescence from intact leaves was measured with a PAM-2000 fluorometer (Walz),
593 as described previously (Ramel et al., 2012b). The maximum quantum yield of PSII was
594 determined by the F_v/F_m ratio, measured in dark-adapted intact leaves. Chlorophyll fluorescence
595 imaging was done with a laboratory-built instrument described in (Johnson et al., 2009).

596

597 **RNA isolation and RT-qPCR**

598 Total RNA was isolated from 150 mg leaves, deriving from a pool of the shoots of 3 plants for each
599 condition, using the Nucleospin RNA Plant kit (Macherey-Nagel). The concentration was
600 measured on a NanoDrop2000 (Thermo Scientific, USA). First strand cDNA was synthesized from
601 3 µg total RNA using the PrimeScript Reverse Transcriptase kit (Takara, Japan). RT-qPCR was
602 performed on a Lightcycler 480 Real-Time PCR system (Roche, Switzerland). 3 µl of a reaction
603 mixture comprising SYBR Green I Master (Roche, Switzerland), 10 µM each of forward and reverse
604 primers and water, was added to 2 µL of a 50-fold diluted cDNA sample in a 384 well plate. Each
605 condition was represented by 4 technical replicates. The PCR program used was: 95 °C for 10 min,
606 then 45 cycles of 95 °C for 15 s, 58 °C for 15 s and 72 °C for 15 s. Primers for all genes examined
607 (Table S1) were designed using the Primer-BLAST software

608 (<https://www.ncbi.nlm.nih.gov/tools/primer-blast/>). *PROFILIN-1* and *CYCLOPHYLIN-5* were used
609 as reference genes for the normalization of gene expression levels.

610
611 **β -glucuronidase histochemical assay**
612 Histochemical staining was performed on 5-week-old plants of the ANAC102-GUS translational
613 reporter. Samples, belonging to two transgenic lines, were analyzed for β -glucuronidase activity
614 by observing the specific blue staining. Samples were incubated overnight at 37 °C in the reaction
615 medium (1mM X-Gluc, 0.05% Triton X-100, 1 mM $K_3Fe(CN)_6$, 1 mM $K_4Fe(CN)_6 \cdot 3 \times H_2O$, 10mM
616 EDTA, and 50mM sodium phosphate buffer, pH 7.0).

617
618 **Detection of ROS Production**
619 1O_2 or H_2O_2 production was measured in attached leaves respectively by using the SOSG or the
620 H2DCFDA fluorescent probe (Invitrogen) (Flors et al., 2006), as previously described (Ramel et al.,
621 2012a). Leaves were infiltrated with 100mM probe by a 1-mL syringe, without needle. Plants were
622 exposed for 4 hours to a PFD of 1500 $\mu mol m^{-2} s^{-1}$ at 7°C then infiltrated and put further 30 min
623 under stress conditions. SOSG fluorescence was then measured using a Perkin-Elmer
624 Spectrofluorometer (LS 50B) at 515 nm with a 475-nm excitation. H2DCFDA fluorescence was
625 measured at 525 nm with a 490-nm exciting light beam.

626
627 **Statistics**
628 All experiments were performed at least on three biological replicates, and the images represent
629 typical examples. Each experiment included the corresponding independent control. The values
630 are represented as the means + standard deviation. The statistical significance was tested using
631 Student's *t*-test (two-tailed, unequal variances).

632
633 **Accession Numbers**
634 Sequence data from this article can be found in the Arabidopsis Genome Initiative or GenBank/EMBL
635 databases under the following accession numbers:

636 *MBS1* (AT3G02790), *SCL14* (AT1G07530), *ANAC102* (AT5G63790), *ANAC002* (AT1G01720), *ANAC032*
637 (AT1G77450), *ANAC081* (AT5G08790).

638

639 **Supplemental Data**

640 Supplemental Figure 1: β -cc induction of *ANAC* genes is independent of NPR1.

641 Supplemental Figure 2: Effect of cycloheximide on *ANAC102* induction by β -cc.

642 Supplemental Figure 3: The resilience of young leaves to excessive light depends on SCL14.

643 Supplemental Table 1: Primers used in the work

644

645 **FUNDINGS**

646 This work was supported by a grant from the French National Research Agency (ANR project
647 SLOSAM, 14-CE02-0010-02).

648

649 **AUTHOR CONTRIBUTIONS**

650 S.D and M.H. conceived the study, S.D. performed most experiments, B. K. performed HOTE
651 quantifications, S.D. and M.H. analyzed the data and wrote the article.

652

653 **ACKNOWLEDGMENTS**

654 We would like to thank the Phytotec platform (CEA Cadarache) for growing plants under control
655 and stress conditions. We are also thankful to C. Gatz (Gottingen, Germany) for the kind gift of
656 seeds of the *tgall* and of the *scl14* knock-out mutant and the *SCL14* overexpressor. We would
657 thank Dr. G. Bethke (St.Paul, Minnesota) for the kind gift of the *npr1* mutant seeds. Finally, we
658 thank Dr. X. Johnson (CEA Cadarache) for help with chlorophyll fluorescence imaging and for
659 careful reading of the manuscript.

660

661

662 **REFERENCES**

663

664 **Apel, K. and Hirt, H.** (2004). REACTIVE OXYGEN SPECIES: Metabolism, Oxidative Stress, and
665 Signal Transduction. *Annu. Rev. Plant Biol.* **55**: 373–399.

666 **Asada, K.** (2006). Production and Scavenging of Reactive Oxygen Species in Chloroplasts and

667 Their Functions. *Plant Physiol.* **141**: 391–396.

668 **Bielczynski, L.W., Łacki, M.K., Hoefnagels, I., Gambin, A., and Croce, R.** (2017). Leaf and Plant
669 Age Affects Photosynthetic Performance and Photoprotective Capacity. *Plant Physiol.* **175**:
670 1634–1648.

671 **Birtic, S., Ksas, B., Genty, B., Mueller, M.J., Triantaphylidès, C., and Havaux, M.** (2011). Using
672 spontaneous photon emission to image lipid oxidation patterns in plant tissues. *Plant J.* **67**:
673 1103–1115.

674 **Carmody, M., Crisp, P.A., D’Alessandro, S., Ganguly, D., Gordon, M., Havaux, M., Albrecht-
675 Borth, V., and Pogson, B.J.** (2016). Uncoupling High Light Responses from Singlet Oxygen
676 Retrograde Signaling and Spatial-Temporal Systemic Acquired Acclimation. *Plant Physiol.*
677 **171**: 1734–1749.

678 **Chan, K.X., Phua, S.Y., Crisp, P., McQuinn, R., and Pogson, B.J.** (2016). Learning the Languages
679 of the Chloroplast: Retrograde Signaling and Beyond. *Annu. Rev. Plant Biol.* **67**: 25–53.

680 **Chini, A., Fonseca, S., Fernández, G., Adie, B., Chico, J.M., Lorenzo, O., García-Casado, G.,
681 López-Vidriero, I., Lozano, F.M., Ponce, M.R., Micol, J.L., and Solano, R.** (2007). The JAZ
682 family of repressors is the missing link in jasmonate signalling. *Nature* **448**: 666–671.

683 **Christianson, J.A., Wilson, I.W., Llewellyn, D.J., and Dennis, E.S.** (2009). The Low-Oxygen-
684 Induced NAC Domain Transcription Factor ANAC102 Affects Viability of Arabidopsis Seeds
685 following Low-Oxygen Treatment. *Plant Physiol.* **149**: 1724–1738.

686 **DeRidder, B.P., Dixon, D.P., Beussman, D.J., Edwards, R., and Goldsbrough, P.B.** (2002).
687 Induction of glutathione S-transferases in Arabidopsis by herbicide safeners. *Plant Physiol.*
688 **130**: 1497–1505.

689 **Després, C., DeLong, C., Glaze, S., Liu, E., and Fobert, P.R.** (2000). The Arabidopsis NPR1/NIM1
690 Protein Enhances the DNA Binding Activity of a Subgroup of the TGA Family of bZIP
691 Transcription Factors. *Plant Cell* **12**: 279–290.

692 **Fan, W. and Dong, X.** (2002). In Vivo Interaction between NPR1 and Transcription Factor TGA2
693 Leads to Salicylic Acid-Mediated Gene Activation in Arabidopsis. *Plant Cell* **14**: 1377–1389.

694 **Farmer, E.E. and Mueller, M.J.** (2013). ROS-Mediated Lipid Peroxidation and RES-Activated
695 Signaling. *Annu. Rev. Plant Biol.* **64**: 429–450.

696 **Flors, C., Fryer, M.J., Waring, J., Reeder, B., Bechtold, U., Mullineaux, P.M., Nonell, S., Wilson,
697 M.T., and Baker, N.R.** (2006). Imaging the production of singlet oxygen in vivo using a new
698 fluorescent sensor, Singlet Oxygen Sensor Green®. *J. Exp. Bot.* **57**: 1725–1734.

699 **Fode, B., Siemsen, T., Thurow, C., Weigel, R., and Gatz, C.** (2008). The Arabidopsis GRAS Protein
700 SCL14 Interacts with Class II TGA Transcription Factors and Is Essential for the Activation of
701 Stress-Inducible Promoters. *Plant Cell* **20**: 3122–3135.

702 **Frank, H.A. and Cogdell, R.J.** (1996). Carotenoids in Photosynthesis. *Photochem. Photobiol.* **63**:
703 257–264.

704 **Gadjev, I.** (2006). Transcriptomic Footprints Disclose Specificity of Reactive Oxygen Species
705 Signaling in Arabidopsis. *Plant Physiol.* **141**: 436–445.

706 **Havaux, M.** (2014). Carotenoid oxidation products as stress signals in plants. *Plant J.* **79**: 597–
707 606.

708 **Huang, L.-J., Li, N., Thurow, C., Wirtz, M., Hell, R., and Gatz, C.** (2016). Ectopically expressed
709 glutaredoxin ROXY19 negatively regulates the detoxification pathway in Arabidopsis
710 thaliana. *BMC Plant Biol.* **16**: 200–211.

711 **Johnson, X., Vandystadt, G., Bujaldon, S., Wollman, F.A., Dubois, R., Roussel, P., Alric, J., and
712 Béal, D.** (2009). A new setup for in vivo fluorescence imaging of photosynthetic activity.
713 *Photosynth. Res.* **102**: 85–93.

714 **Karimi, M., Inzé, D., and Depicker, A.** (2002). GATEWAY™ vectors for Agrobacterium-mediated
715 plant transformation. *Trends Plant Sci.* **7**: 193–195.

716 **Katagiri, F., Lam, E., and Chua, N.-H.** (1989). Two tobacco DNA-binding proteins with homology

717 to the nuclear factor CREB. *Nature* **340**: 727–730.

718 **Kesarwani, M., Yoo, J., and Dong, X.** (2007). Genetic Interactions of TGA Transcription Factors
719 in the Regulation of Pathogenesis-Related Genes and Disease Resistance in Arabidopsis.
720 *Plant Physiol.* **144**: 336–346.

721 **Köster, J., Thurow, C., Kruse, K., Meier, A., Iven, T., Feussner, I., and Gatz, C.** (2012).
722 Xenobiotic- and Jasmonic Acid-Inducible Signal Transduction Pathways Have Become
723 Interdependent at the Arabidopsis CYP81D11 Promoter. *Plant Physiol.* **159**: 391–402.

724 **Kotchoni, S.O., Kuhns, C., Ditzer, A., Kirch, H.H., and Bartels, D.** (2006). Over-expression of
725 different aldehyde dehydrogenase genes in Arabidopsis thaliana confers tolerance to
726 abiotic stress and protects plants against lipid peroxidation and oxidative stress. *Plant, Cell*
727 *Environ.* **29**: 1033–1048.

728 **Kouřil, R., Wientjes, E., Bultema, J.B., Croce, R., and Boekema, E.J.** (2013). High-light vs. low-
729 light: Effect of light acclimation on photosystem II composition and organization in
730 Arabidopsis thaliana. *Biochim. Biophys. Acta - Bioenerg.* **1827**: 411–419.

731 **Kreuz, K., Tommasini, R., and Martinoia, E.** (1996). Old enzymes for a new job. Herbicide
732 detoxification in plants. *Plant Physiol.* **111**: 349–353.

733 **Krieger-Liszkay, A., Fufezan, C., and Trebst, A.** (2008). Singlet oxygen production in
734 photosystem II and related protection mechanism. *Photosynth. Res.* **98**: 551–64.

735 **Lam, E. and Lam, Y. kam P.** (1995). Binding site requirements and differential representation of
736 TGA factors in nuclear ASF-1 activity. *Nucleic Acids Res.* **23**: 3778–3785.

737 **Li, Z., Wakao, S., Fischer, B.B., and Niyogi, K.K.** (2009). Sensing and Responding to Excess Light.
738 *Annu. Rev. Plant Biol.* **60**: 239–260.

739 **Mano, J.** (2012). Reactive carbonyl species: Their production from lipid peroxides, action in
740 environmental stress, and the detoxification mechanism. *Plant Physiol. Biochem.* **59**: 90–
741 97.

742 **Mano, J., Belles-Boix, E., Babiychuk, E., Inzé, D., Torii, Y., Hiraoka, E., Takimoto, K., Slooten, L.,**
743 **Asada, K., and Kushnir, S.** (2005). Protection against photooxidative injury of tobacco
744 leaves by 2-alkenal reductase. Detoxication of lipid peroxide-derived reactive carbonyls.
745 *Plant Physiol.* **139**: 1773–83.

746 **Matsuo, M., Johnson, J.M., Hieno, A., Tokizawa, M., Nomoto, M., Tada, Y., Godfrey, R.,**
747 **Obokata, J., Sherameti, I., Yamamoto, Y.Y., Böhmer, F.D., and Oelmüller, R.** (2015). High
748 REDOX RESPONSIVE TRANSCRIPTION FACTOR1 Levels Result in Accumulation of Reactive
749 Oxygen Species in *Arabidopsis thaliana* Shoots and Roots. *Mol. Plant* **8**: 1253–1273.

750 **Montillet, J.L. et al.** (2013). An Abscisic Acid-Independent Oxylipin Pathway Controls Stomatal
751 Closure and Immune Defense in *Arabidopsis*. *PLoS Biol.* **11**: e1001513.

752 **Montillet, J.L., Cacas, J.L., Garnier, L., Montané, M.H., Douki, T., Bessoule, J.J., Polkowska-**
753 **Kowalczyk, L., Maciejewska, U., Agnel, J.P., Vial, A., and Triantaphylidès, C.** (2004). The
754 upstream oxylipin profile of *Arabidopsis thaliana*: A tool to scan for oxidative stresses. *Plant*
755 *J.* **40**: 439–451.

756 **Mousavi, S.A.R., Chauvin, A., Pascaud, F., Kellenberger, S., and Farmer, E.E.** (2013).
757 GLUTAMATE RECEPTOR-LIKE genes mediate leaf-to-leaf wound signalling. *Nature* **500**: 422.

758 **Moustaka, J., Tanou, G., Adamakis, I.D., Eleftheriou, E.P., and Moustakas, M.** (2015). Leaf age-
759 dependent photoprotective and antioxidative response mechanisms to paraquat-induced
760 oxidative stress in *arabidopsis thaliana*. *Int. J. Mol. Sci.* **16**: 13989–14006.

761 **Mueller, M.J. and Berger, S.** (2009). Reactive electrophilic oxylipins: Pattern recognition and
762 signalling. *Phytochemistry* **70**: 1511–1521.

763 **Mueller, S., Hilbert, B., Dueckershoff, K., Roitsch, T., Krischke, M., Mueller, M.J., and Berger, S.**
764 (2008). General Detoxification and Stress Responses Are Mediated by Oxidized Lipids
765 through TGA Transcription Factors in *Arabidopsis*. *Plant Cell* **20**: 768–785.

766 **Ndamukong, I., Abdallat, A. Al, Thurow, C., Fode, B., Zander, M., Weigel, R., and Gatz, C.**
767 (2007). SA-inducible *Arabidopsis* glutaredoxin interacts with TGA factors and suppresses JA-

768 responsive PDF1.2 transcription. *Plant J.* **50**: 128–139.

769 **Oguchi, R., Hikosaka, K., and Hirose, T.** (2003). Does the photosynthetic light-acclimation need
770 change in leaf anatomy? *Plant, Cell Environ.* **26**: 505–512.

771 **Ort, D.R.** (2001). When there is too much light regulate thermal dissipation of excess regulating
772 thermal energy dissipation. *Plant Physiol.* **125**: 29–32.

773 **Ramel, F., Birtic, S., Cuine, S., Triantaphylides, C., Ravanat, J.-L., and Havaux, M.** (2012a).
774 Chemical Quenching of Singlet Oxygen by Carotenoids in Plants. *Plant Physiol.* **158**: 1267–
775 1278.

776 **Ramel, F., Birtic, S., Ginies, C., Soubigou-Taconnat, L., Triantaphylides, C., and Havaux, M.**
777 (2012b). Carotenoid oxidation products are stress signals that mediate gene responses to
778 singlet oxygen in plants. *Proc. Natl. Acad. Sci.* **109**: 5535–5540.

779 **Ramel, F., Ksas, B., Akkari, E., Mialoundama, A.S., Monnet, F., Krieger-Liszkay, A., Ravanat, J.-**
780 **L., Mueller, M.J., Bouvier, F., and Havaux, M.** (2013a). Light-Induced Acclimation of the
781 *Arabidopsis chlorina1* Mutant to Singlet Oxygen. *Plant Cell* **25**: 1445–1462.

782 **Ramel, F., Ksas, B., Akkari, E., Mialoundama, A.S., Monnet, F., Krieger-Liszkay, A., Ravanat, J.-**
783 **L., Mueller, M.J., Bouvier, F., and Havaux, M.** (2013b). Light-Induced Acclimation of the
784 *Arabidopsis chlorina1* Mutant to Singlet Oxygen. *Plant Cell* **25**: 1445–1462.

785 **Ramel, F., Sulmon, C., Serra, A.A., Gouesbet, G., and Couée, I.** (2012c). Xenobiotic sensing and
786 signalling in higher plants. *J. Exp. Bot.* **63**: 3999–4014.

787 **Ratnakaran, N.** (2014). Identification of the role of *Arabidopsis* ATAF-type NAC transcription
788 factors in plant stress and development. (Ph.D. Dissertation). Georg-August University
789 School of Science: <https://ediss.uni-goettingen.de/handle/11858/00-17>.

790 **Redman, J., Whitcraft, J., Johnslon, C., and Arias, J.** (2002). Abiotic and biotic stress
791 differentially stimulate as-1 element activity in *Arabidopsis*. *Plant Cell Rep.* **21**: 180–185.

792 **Riechers, D.E., Kreuz, K., and Zhang, Q.** (2010). Detoxification without Intoxication: Herbicide

793 Safeners Activate Plant Defense Gene Expression. *Plant Physiol.* **153**: 3–13.

794 **Roach, T., Baur, T., Stögl, W., and Krieger-Liszkay, A.** (2017). *Chlamydomonas reinhardtii*
795 responding to high light: a role for 2-propenal (acrolein). *Physiol. Plant.* **161**: 75–87.

796 **Rossel, J.B., Wilson, P.B., Hussain, D., Woo, N.S., Gordon, M.J., Mewett, O.P., Howell, K.A.,**
797 **Whelan, J., Kazan, K., and Pogson, B.J.** (2007). Systemic and Intracellular Responses to
798 Photooxidative Stress in Arabidopsis. *Plant Cell* **19**: 4091–4110.

799 **Sandermann, H.** (1992). Plant metabolism of xenobiotics. *Trends Biochem. Sci.* **17**: 82–84.

800 **Shumbe, L., Bott, R., and Havaux, M.** (2014). Dihydroactinidiolide, a high light-induced β -
801 carotene derivative that can regulate gene expression and photoacclimation in
802 Arabidopsis. *Mol. Plant* **7**: 1248–1251.

803 **Shumbe, L., D’Alessandro, S., Shao, N., Chevalier, A., Ksas, B., Bock, R., and Havaux, M.** (2017).
804 METHYLENE BLUE SENSITIVITY 1 (MBS1) is required for acclimation of Arabidopsis to
805 singlet oxygen and acts downstream of β -cyclocitral. *Plant Cell Environ.* **40**: 216–226.

806 **Sims, D.A. and Percy, R.W.** (1992). Response of Leaf Anatomy and Photosynthetic Capacity in
807 *Alocasia macrorrhiza* (Araceae) to a Transfer from Low to High Light. *Am. J. Bot.* **79**: 449.

808 **Skipsey, M., Knight, K.M., Brazier-Hicks, M., Dixon, D.P., Steel, P.G., and Edwards, R.** (2011).
809 Xenobiotic responsiveness of Arabidopsis thaliana to a chemical series derived from a
810 herbicide safener. *J. Biol. Chem.* **286**: 32268–32276.

811 **Steffens, N.O.** (2004). AthaMap: an online resource for in silico transcription factor binding sites
812 in the Arabidopsis thaliana genome. *Nucleic Acids Res.* **32**: 368–372.

813 **Stiti, N., Missihoun, T.D., Kotchoni, S.O., Kirch, H.-H., and Bartels, D.** (2011). Aldehyde
814 Dehydrogenases in Arabidopsis thaliana: Biochemical Requirements, Metabolic Pathways,
815 and Functional Analysis. *Front. Plant Sci.* **2**: 65.

816 **Taylor, V.L., Cummins, I., Brazier-Hicks, M., and Edwards, R.** (2013). Protective responses
817 induced by herbicide safeners in wheat. *Environ. Exp. Bot.* **88**: 93–99.

818 **Triantaphylidès, C. and Havaux, M.** (2009). Singlet oxygen in plants: production, detoxification
819 and signaling. *Trends Plant Sci.* **14**: 219–228.

820 **Turóczy, Z., Kis, P., Török, K., Cserháti, M., Lendvai, Á., Dudits, D., and Horváth, G. V.** (2011).
821 Overproduction of a rice aldo-keto reductase increases oxidative and heat stress tolerance
822 by malondialdehyde and methylglyoxal detoxification. *Plant Mol. Biol.* **75**: 399–412.

823 **De Veylder, L., Van Montagu, M., and Inze, D.** (1997). Herbicide safener-inducible gene
824 expression in *Arabidopsis thaliana*. *Plant Cell Physiol* **38**: 568–577.

825 **Wagner, D., Przybyla, D., op den Camp, R., Kim, C., Landgraf, F., Lee, K.P., Wursch, M., Laloi,**
826 **C., Nater, M., Hideg, E., and Apel, K.** (2004). The Genetic Basis of Singlet Oxygen-Induced
827 Stress Responses of *Arabidopsis thaliana*. *Science* (80-.). **306**: 1183–1185.

828 **Yamauchi, Y., Hasegawa, A., Taninaka, A., Mizutani, M., and Sugimoto, Y.** (2011). NADPH-
829 dependent reductases involved in the detoxification of reactive carbonyls in plants. *J. Biol.*
830 *Chem.* **286**: 6999–7009.

831 **Zhou, J.-M., Trifa, Y., Silva, H., Pontier, D., Lam, E., Shah, J., and Klessig, D.F.** (2000). NPR1
832 Differentially Interacts with Members of the TGA/OBF Family of Transcription Factors That
833 Bind an Element of the PR-1 Gene Required for Induction by Salicylic Acid. *Mol. Plant-*
834 *Microbe Interact.* **13**: 191–202.

835

836

837

838

839

840 **Figure legends:**

841 **Figure 1: β -cyclocitral elicits a SCL14-like response involving the TGA and MYC transcription**
842 **factors**

843 (A) Number of genes whose expression increases or decreases more than 1.5 fold in \log_2 values
844 compared to the respective controls in the transcriptome of β -cyclocitral-treated wt plants (4h
845 treatment, β -cc) and of the *ch1* mutant line under high light stress (*ch1* HL, 1200 $\mu\text{mol photons}$
846 $\text{m}^{-2} \text{s}^{-1}$ at 10°C for 24h). (B) Transcription factors cis element enrichment in the regulatory regions
847 (-1000 + 50 base pairs from the starting codon) of the common genes. (C) *ANAC002*, *ANAC032*,
848 *ANAC081* and *ANAC102* expression levels (fold-change relative to the control levels) in wild type
849 plants exposed to β -cc or under excessive light stress (HL), measured by RT-qPCR. Every value
850 showed a significant difference when tested against CTRL conditions ($P < 0.01$). Error bars = + SD
851 between the four technical replicates from pools of three plants per treatment. Two full
852 experimental replicates.

853

854 **Figure 2: β -cyclocitral induces SCL14 and the downstream response**

855 *ANAC002*, *ANAC032*, *ANAC081*, *ANAC102* and *SCL14* expression levels (relative to wt control
856 levels, WT CTRL, which are set to 1) in wt, *scl14*, *tga II* and OE:SCL14 plants under control
857 conditions or exposed to β -cc, measured by RT-qPCR. ANAC genes induced by β -cc in the
858 OE:SCL14, *scl14* and *tga II* plants showed a significant difference when tested against β -cc
859 induction in the wt ($P < 0.01$). The black diamonds indicate expression levels significantly different
860 from *SCL14* expression levels in the corresponding control condition ($P < 0.01$). Error bars = + SD
861 between the four technical replicates from pools of three plants per genotype per treatment.

862

863 **Figure 3: *scl14* mutant lines are not able to acquire β -cc-induced resistance to excessive light**

864 (A) Leaf bleaching (top panel) and lipid peroxidation, monitored by autoluminescence imaging
865 (bottom of panel), of wt, *scl14* and OE:SCL14 plants pre-treated with β -cc or with water. The color
866 palette shows signal intensity from low (dark blue) to high (white) values. (B) HPLC-UV
867 quantification of the HOTE normalized to the wt control (CTRL). The black diamonds indicate

868 significant differences with $P < 0.05$. Error bars = + SD between the technical replicates from pools
869 of three plants. Error bars = + SD between the four biological replicates from leaves of three plants
870 per genotype per treatment. Two full experimental replicates.

871
872 **Figure 4: *tga II* mutant lines are sensitive to excessive light and unresponsive to β -cc**
873 (A) Leaf bleaching (top panel) and lipid peroxidation, monitored by autoluminescence imaging
874 (bottom panel), of wt and of *tga II* mutant plants pre-treated with β -cc or with water. The color
875 palette shows signal intensity from low (dark blue) to high (white) values. (B) HPLC-UV
876 quantification of the HOTE normalized on wt control (CTRL). The black diamonds indicate
877 significant differences with $P < 0.05$. Error bars = + SD between the four biological replicates from
878 leaves of three plants per genotype per treatment. Two full experimental replicates.

879
880 **Figure 5: β -cyclocitral induces a SCL14-dependent xenobiotic-detoxification response**
881 *SDR1*, *ChiADR*, *AKR4C9*, *AER*, *GRX480/ROXY19* and *AT5G61820* expression levels (relative to wt
882 control levels, WT CTRL, which are set to 1) in wt, *scl14*, *tga II* and OE:SCL14 plants under control
883 conditions or exposed to β -cc, measured by RT-qPCR. Every gene induced by β -cc in the OE:SCL14,
884 *scl14* and *tga II* plants showed a significant difference when tested against β -cc induction in the
885 wt ($P < 0.01$). Error bars = + SD between the four technical replicates from pools of three plants
886 per genotype per treatment.

887
888 **Figure 6: *anac102* mutant lines are sensitive to excessive light and unresponsive to β -cc**
889 (A) Leaf bleaching (top panel) and lipid peroxidation, monitored by autoluminescence imaging
890 (bottom panel), of wt and of *anac102* mutant plants pre-treated with β -cc or with water. The
891 color palette shows signal intensity from low (dark blue) to high (white) values. (B) HPLC-UV
892 quantification of the HOTE normalized to wt control (CTRL). The black diamonds indicate
893 significant differences with $P < 0.05$. Error bars = + SD between the technical replicates from pools
894 of three plants. Error bars = + SD between the three biological replicates from leaves of three
895 plants per genotype per treatment. Two full experimental replicates.

896

897 **Figure 7: β -cyclocitral induced SCL14-dependent detoxification response is blocked in *anac102***
898 *SDR1, ChiADR, AKR4C9, AER, GRX480/ROXY19* and *AT5G61820* expression levels (relative to wt
899 control levels, WT CTRL, which were set to 1) in wt, and *anac102* plants under control conditions
900 or exposed to β -cc, measured by RT-qPCR. Every gene induced by β -cc in the *anac102* plants
901 showed a significant difference when tested against β -cc induction in the wt ($P < 0.01$). Error bars
902 = + SD between the four technical replicates from pools of three plants per genotype per
903 treatment.

904
905 **Figure 8: ANAC102 is upstream of ANAC002, ANAC032 and ANAC081**
906 *ANAC002, ANAC032 and ANAC081* expression levels (relative to wt control levels, WT CTRL, which
907 were set to 1) in wt and *anac102* plants under control conditions or exposed to β -cc, measured
908 by RT-qPCR. Every gene induced by β -cc in *anac102* plants showed a significant difference when
909 tested against β -cc induction in the wt ($P < 0.01$). Error bars = + SD between the four technical
910 replicates from pools of three plants per genotype per treatment.

911
912 **Figure 9: SCL14-dependent detoxification pathway is independent of MBS1**
913 *MBS1, ANAC102, ANAC032, AER, SDR1, ChiADR, AKR4C9* and *AT5G61820* expression levels
914 (relative to wt control levels, CTRL, which were set to 1) in wt, and *mbs1* plants under control
915 conditions or exposed to β -cc, measured by RT-qPCR. MBS1 expression in the mutant is
916 significantly lower than in wt ($P < 0.01$). *ANAC102, ANAC032, AER, SDR1, ChiADR, AKR4C9* and
917 *AT5G61820* expression levels after β -cc treatment are significantly different from the relative
918 control level in wt or *mbs1* mutant plants ($P > 0.01$). Error bars = + SD between the four technical
919 replicates from pools of three plants per genotype per treatment. Two full experimental replicates

920
921 **Figure 10: ANAC102 is particularly induced in young leaves**
922 (A) Schematization of the ANAC102 translational reporter. (B) Histochemical analyses of the
923 translational reporter after 4h treatment with water (CTRL) or β -cc (β -cc) and overnight
924 development of the staining. Two full experimental replicates.

925

926 **Figure 11: The resilience of young leaves to excessive light depends on SCL14**

927 (A) Leaf bleaching (on the left) and lipid peroxidation monitored by autoluminescence imaging
928 (on the right) of wt, *sc/14* and of OE:SCL14 detached leaves after high light stress. (B) Maximum
929 quantum yield of PSII photochemistry determined by the Fv/Fm chlorophyll fluorescence ratio of
930 wt, *sc/14* and of OE:SCL14 mature and young detached leaves after high light stress. (C) HPLC-UV
931 quantification of the HOTE normalized to wt mature leaves. Black diamonds indicate significant
932 differences ($P < 0.05$). Error bar = + SD between the technical replicates from pools of four mature
933 leaves or ten young leaves. Error bars = + SD between the three biological replicates of pools of
934 four mature leaves or ten young leaves. Two full experimental replicates.

935
936 **Figure 12: SCL14-dependent detoxification pathway acts on toxic RCS rather than on ROS**
937 **accumulation**

938 (A) Leaf bleaching (top panel) and lipid peroxidation, monitored by autoluminescence imaging
939 (bottom panel), of wt plants pre-treated with 1 mM HNE or with water. The color palette shows
940 signal intensity from low (dark blue) to high (white) values. (B) HPLC-UV quantification of the HOTE
941 normalized to the wt control (CTRL). The black diamonds indicate significant differences with $P <$
942 0.05 . Error bar = + SD between the four biological replicates from leaves of three plants per
943 treatment. (C) SOSG or H₂DCFDA fluorescence in wt, *sc/14* or OE:SCL14 plants tested measured
944 after 4h of high light stress. Error bars = + SD between fluorescence deriving from five leaves per
945 plant (Two plants per genotype per treatment).

946
947 **Figure 13. β -cyclocitral Mediates Resilience to Photooxidative Stress via the SCL14-dependent**
948 **Xenobiotic Response**

949 Photo-oxidation under excessive light stress generates toxic RCS metabolites and increases β -cc
950 concentration. β -cc induces the expression of SCL14 leading to enhanced expression of ANAC102
951 and finally a strong activation of the xenobiotic detoxification response. In this response, ANAC102
952 is upstream of ANAC002, ANAC032 and ANAC081 expression, and consequently of the enzymes
953 controlled by these transcription factors. Furthermore, the strong induction of the AER, AKRs,

954 ALDHs and SDRs enzymes and of the glucosyl and glutathione transferases in the xenobiotic
955 detoxification pathway assures the elimination of the RCS produced under stress conditions.
956 Reducing RCS accumulation limits the positive feedback on lipid peroxidation and lead to
957 tolerance rather than cell death.

958

959 **Supplemental Figure 1: β -cc induction of ANAC genes is independent of NPR1.**

960 Supports Figure 2.

961 *PR1*, *ANAC102*, *ANAC032*, *ATAF1/ANAC002* and *ATAF2/ANAC081* expression levels (relative to wt
962 control levels, CTRL, which were set to 1) in wt, and *npr1* plants under control conditions or
963 exposed to β -cc, measured by RT-qPCR. *PR1* expression level in the *npr1* mutant line is significantly
964 lower than in wt ($P < 0,01$). *ANAC102*, *ANAC032*, *ATAF1/ANAC002* and *ATAF2/ANAC081* expression
965 levels in β -cc treated plant are significantly different from expression in the relative wt or *npr1*
966 control ($P < 0,01$). Error bars = + SD between the technical replicates from pools of three plants
967 per genotype per treatment.

968

969 **Supplemental Figure 2: Effect of cycloheximide on ANAC102 induction by β -cc.**

970 Supports Figure 10.

971 The ANAC102 translational reporter described in Figure 10 was used in this experiment. Stain after
972 4-h treatment with water (H_2O), β -cc (β -cc), cycloheximide (CHX) or β -cc and CHX and overnight
973 development of the staining.

974

975

976 **Supplemental Figure 3: The resilience of young leaves to excessive light depends on SCL14.**

977 Supports Figure 11.

978 (A) Leaf bleaching of typical wt, *sc14* and OE:SCL14 plants after high light stress. Leaves were
979 detached from the plants after the stress and placed, by age, on a flat surface from the 4th to the
980 18-20th youngest leaf. (B) Leaf bleaching (on the left) and maximum quantum yield imaging of
981 PSII photochemistry determined by the Fv/Fm chlorophyll fluorescence ratio (on the right) of wt,

982 *sc14* and of OE:SCL14 detached leaves after high light stress. The color palette shows signal
983 intensity from low (dark blue) to high (red) values. (C) Leaf bleaching (on the left) and lipid
984 peroxidation monitored by autoluminescence imaging (on the right) of wt, *sc14* and of OE:SCL14
985 detached leaves after high light stress. The color palette shows signal intensity from low (dark
986 blue) to high (white) values. Two full experimental replicates.

987

988 Supplemental Table 1: Primers used in the work

989

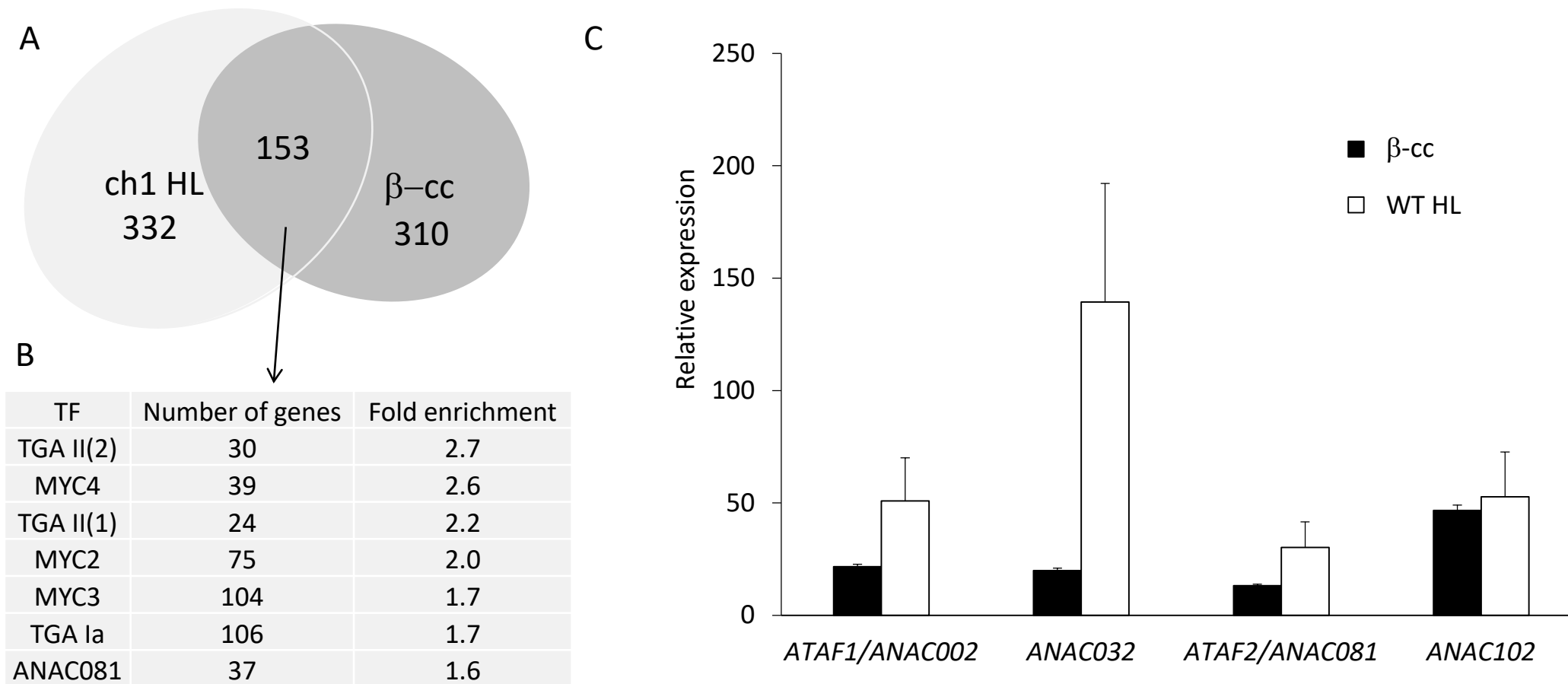


Figure 1: β -cyclocitral elicits a SCL14-like response involving the TGA and MYC transcription factors

(A) Number of genes whose expression increases or decreases more than 1.5 fold in \log_2 values compared to the respective controls in the transcriptome of β -cyclocitral-treated wt plants (4-h treatment, β -cc) and of the *ch1* mutant line under high light stress (*ch1* HL, 1200 $\mu\text{mol photons m}^{-2} \text{s}^{-1}$ at 10°C for 24h). (B) Transcription factors cis element enrichment in the regulative regions (-1000 + 50 base pairs from the starting codon) of the common genes. (C) *ANAC002*, *ANAC032*, *ANAC081* and *ANAC102* expression levels (fold-changes relative to the control levels) in wt plants exposed to β -cc or under excessive light stress (HL), measured by RT-qPCR. Every value showed a significant difference when tested against CTRL conditions ($P < 0.01$). Error bars = + SD between the four technical replicates from pools of three plants per treatment. Two full experimental replicates.

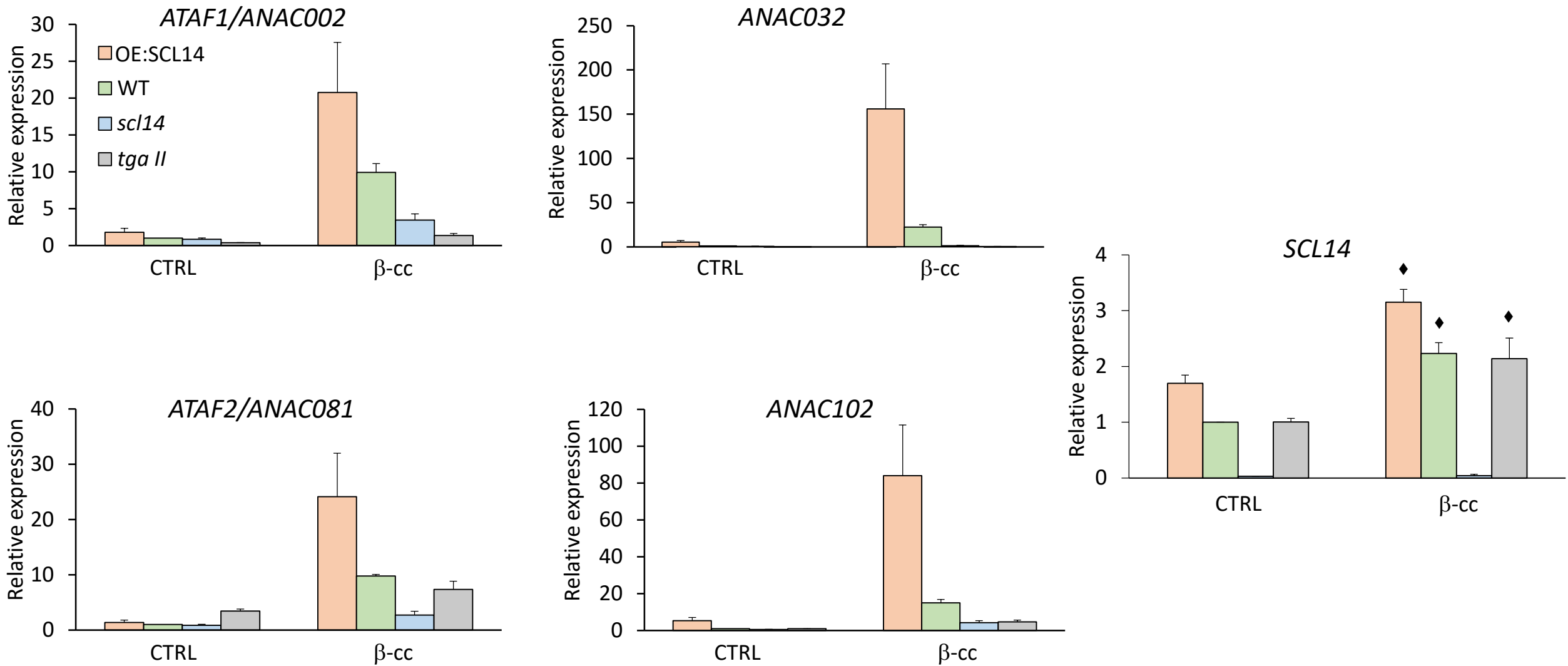


Figure 2: β -cyclocitral induces SCL14 and the downstream response

ANAC002, *ANAC032*, *ANAC081*, *ANAC102* and *SCL14* expression levels (relative to wt control levels, WT CTRL, which was set to 1) in wt, *scl14*, *tga II* and OE:SCL14 plants under control conditions or exposed to β -cc, measured by qRT-PCR. ANAC genes induced by β -cc in the OE:SCL14, *scl14* and *tga II* plants showed a significant difference when tested against β -cc induction in the wt ($P < 0.01$). The black diamonds indicate expression levels significantly different from *SCL14* expression levels in the relative control condition ($P < 0.01$). Error bars = + SD between the four technical replicates from pools of three plants per genotype per treatment.

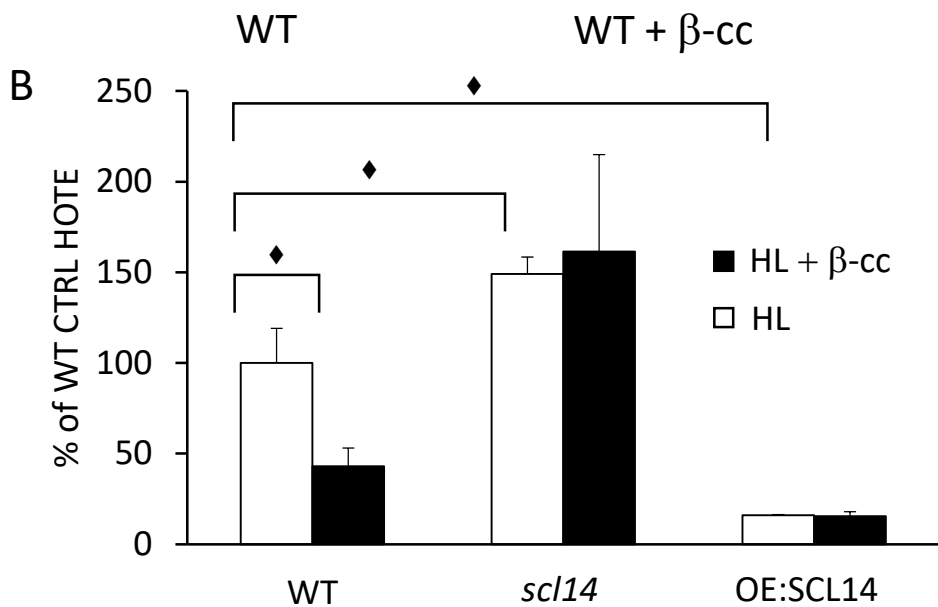
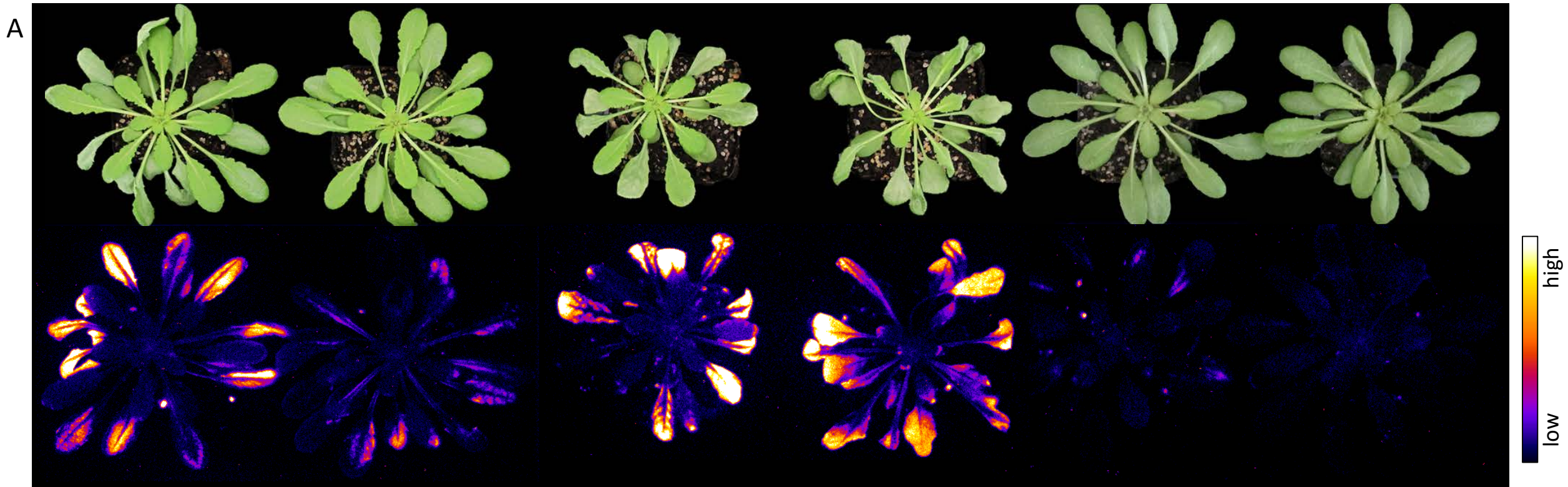


Figure 3: *scl14* mutant lines are not able to acquire β -cc-induced resistance to excessive light

(A) Leaf bleaching (top panel) and lipid peroxidation, monitored by autoluminescence imaging (bottom of panel), of wt *scl14* and OE:SCL14 plants pre-treated with β -cc or with water. The color palette shows signal intensity from low (dark blue) to high (white) values. (B) HPLC-UV quantification of the HOTE normalized to the wt control (CTRL). The black diamonds indicate significant differences with $P < 0.05$. Error bars = + SD between the four biological replicates from leaves of three plants per genotype per treatment. Two full experimental replicates.

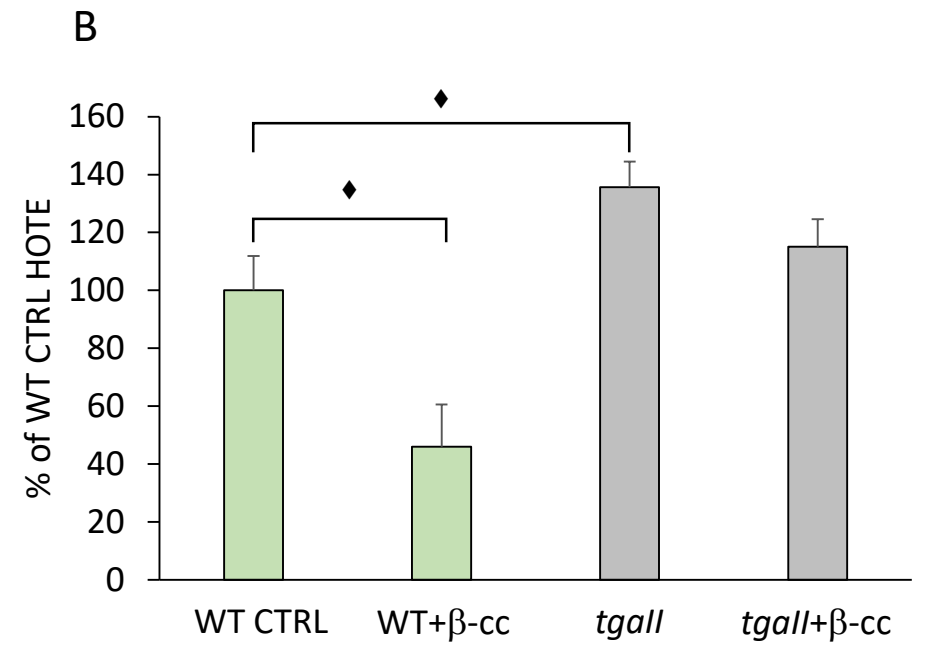
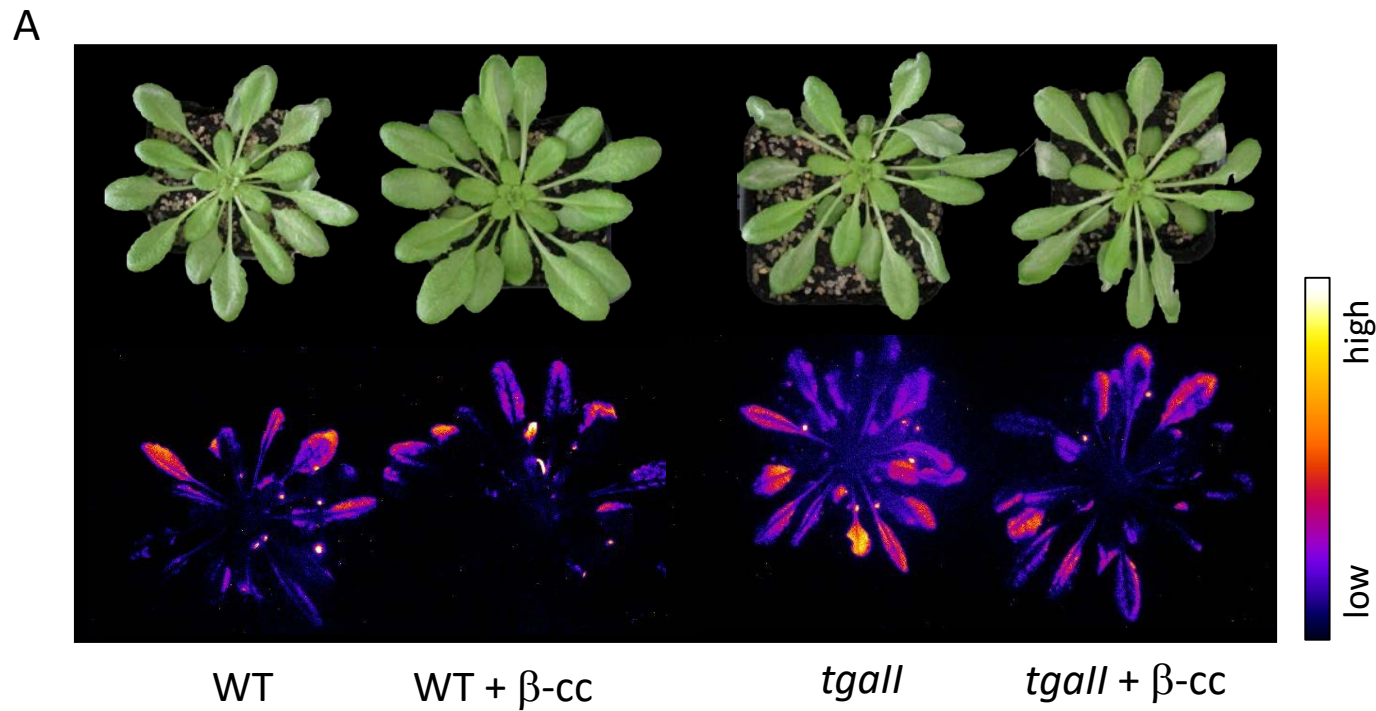


Figure 4: ***tga II* mutant lines are sensitive to excessive light and unresponsive to β -cc**

(A) Leaf bleaching (top panel) and lipid peroxidation, monitored by autoluminescence imaging (bottom panel), of WT and of *tga II* triple mutant plants pre-treated with β -cc or with water. The color palette shows signal intensity from low (dark blue) to high (white) values. (B) HPLC-UV quantification of the HOTE normalized on WT control (CTRL). The black diamonds indicate significant differences with $P < 0.05$. Error bars = + SD between the four biological replicates from leaves of three plants per genotype per treatment. Two full experimental replicates.

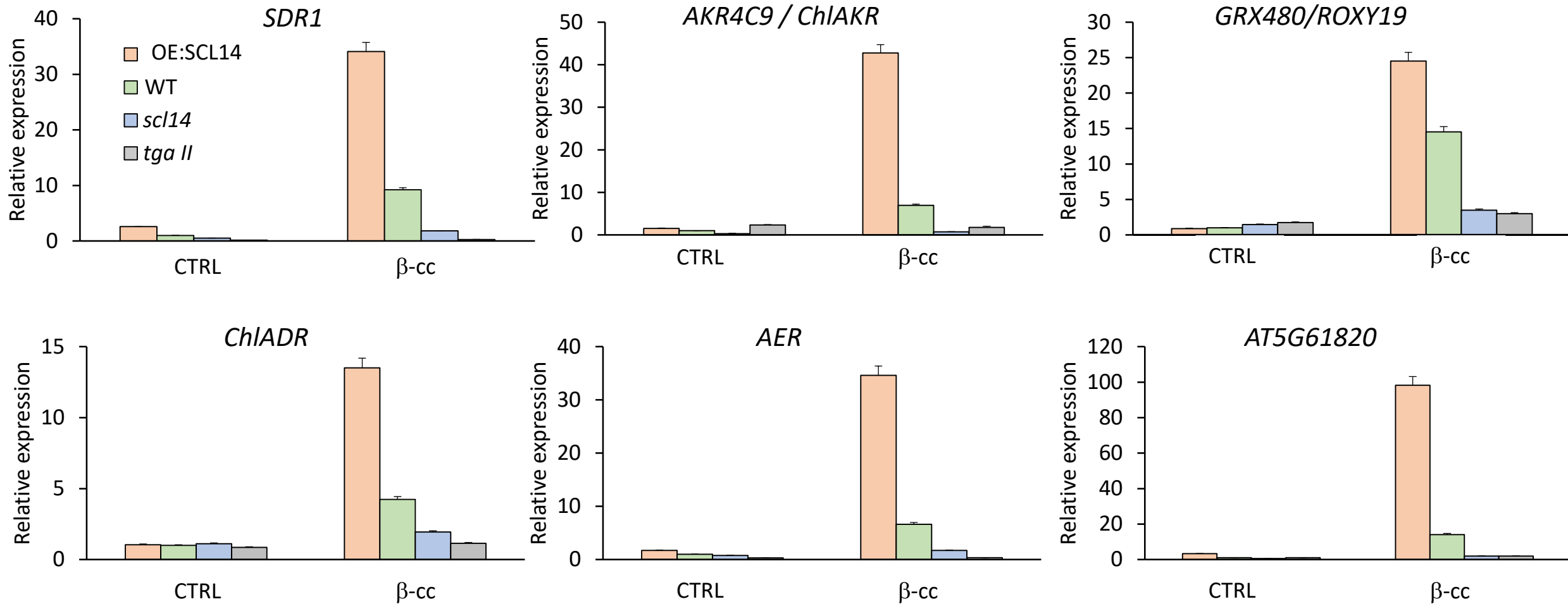
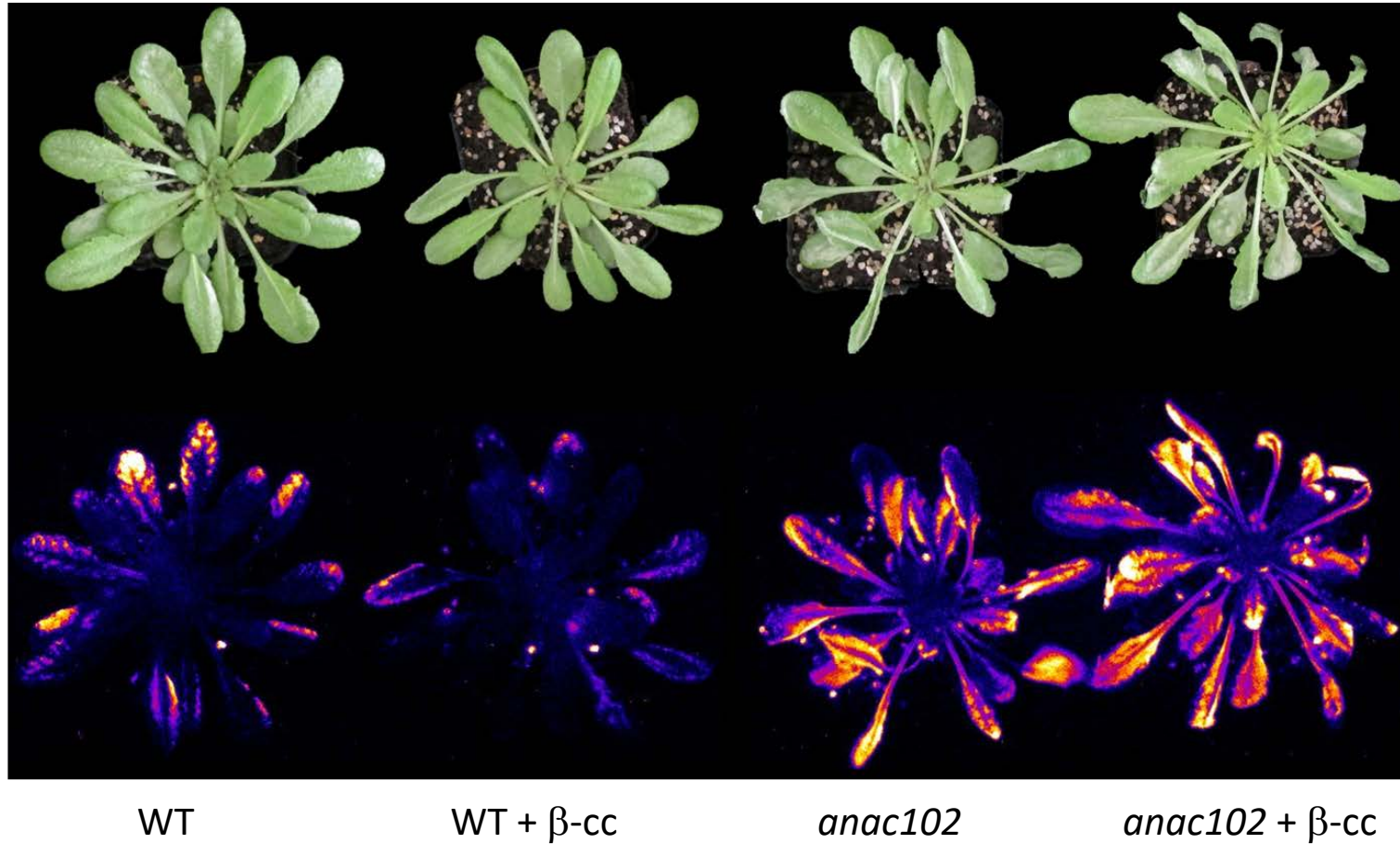


Figure 5: β -cyclocitral induces a SCL14-dependent xenobiotic-detoxification response

SDR1, *ChiADR*, *AKR4C9*, *AER*, *GRX480/ROXY19* and *AT5G61820* expression levels (relative to wt control levels, WT CTRL, which were set to 1) in wt, *scl14*, *tga II* and OE:SCL14 plants under control conditions or exposed to β -cc, measured by RT-qPCR. Every gene induced by β -cc in the OE:SCL14, *scl14* and *tga II* plants showed a significant difference when tested against β -cc induction in the wt ($P < 0.01$). Error bars = + SD between the four technical replicates from pools of three plants per genotype per treatment.

A



B

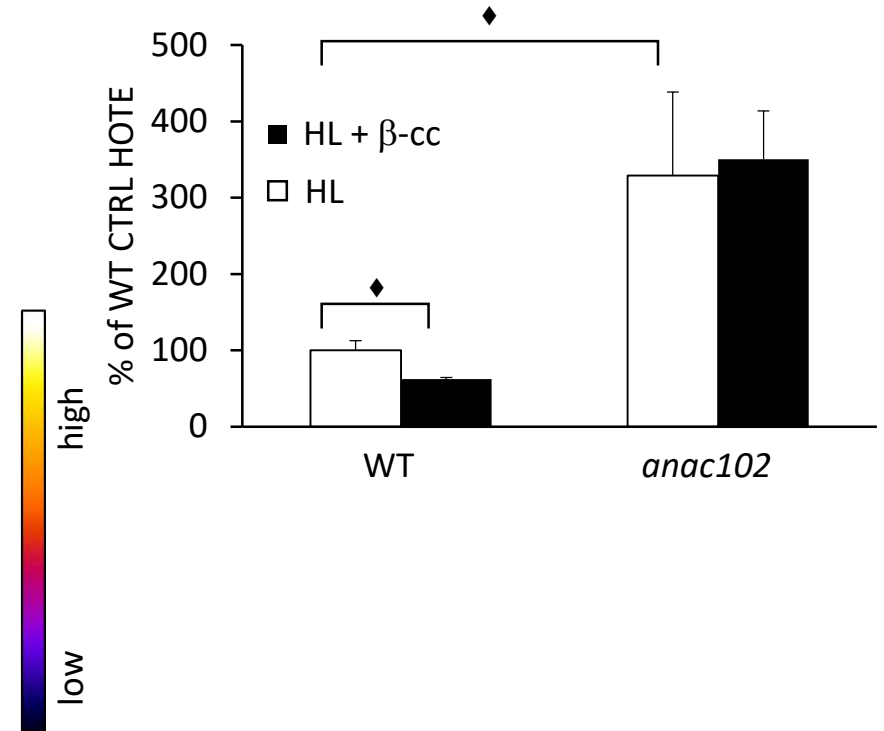


Figure 6: ***anac102* mutant lines are sensitive to excessive light and unresponsive to β -cc**

(A) Leaf bleaching (top panel) and lipid peroxidation, monitored by autoluminescence imaging (bottom panel), of wt and of *anac102* mutant plants pre-treated with β -cc or with water. The color palette shows signal intensity from low (dark blue) to high (white) values. (B) HPLC-UV quantification of the HOTE normalized to the wt control (CTRL). The black diamonds indicate significant differences with $P < 0.05$. Error bars = + SD between the three biological replicates from leaves of three plants per genotype per treatment. Two full experimental replicates.

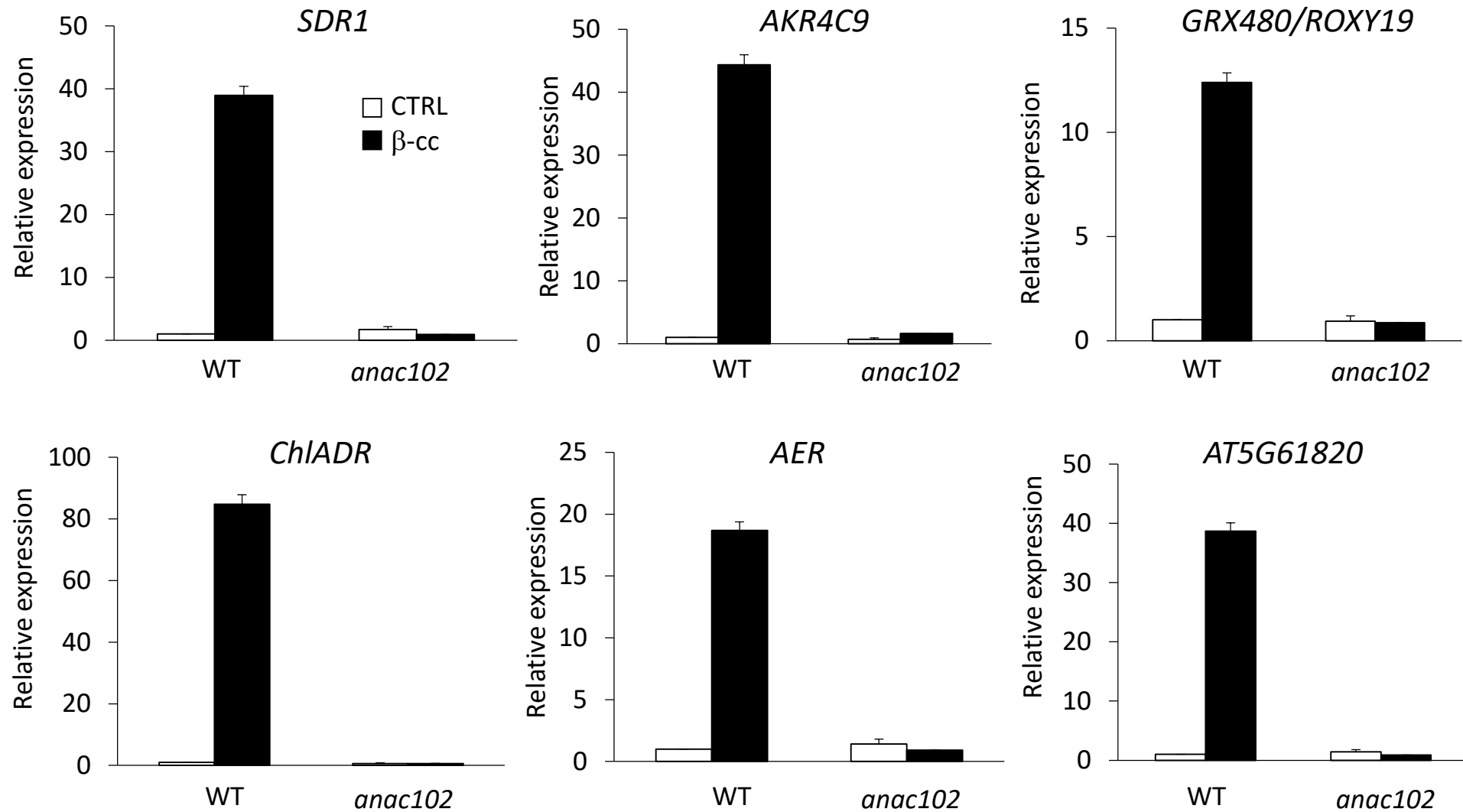


Figure 7: β -cyclocitral-induced SCL14-dependent detoxification response is blocked in *anac102*

SDR1, *ChiADR*, *AKR4C9*, *AER*, *GRX480/ROXY19* and *AT5G61820* expression levels (relative to wt control levels, WT CTRL, which were set to 1) in wt, and *anac102* plants under control conditions or exposed to β -cc, measured by qRT-PCR. Every gene induced by β -cc in the *anac102* plants showed a significant difference when tested against β -cc induction in the wt ($P < 0.01$). Error bars = + SD between the four technical replicates from pools of three plants per genotype per treatment.

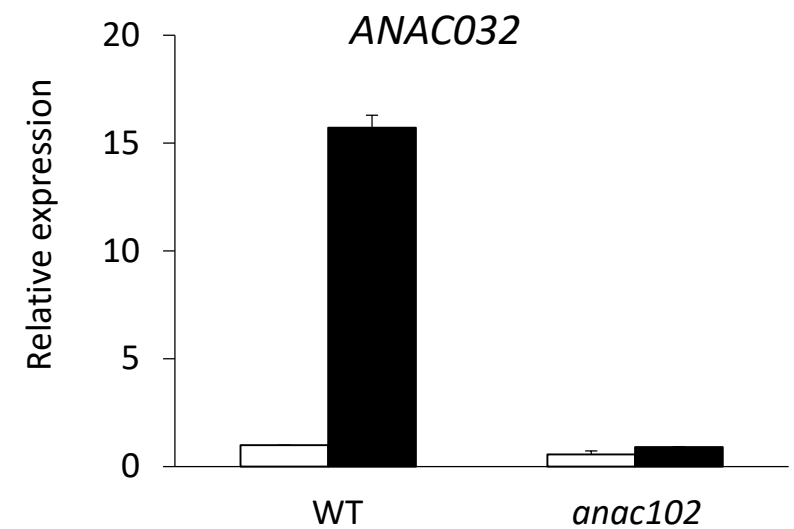
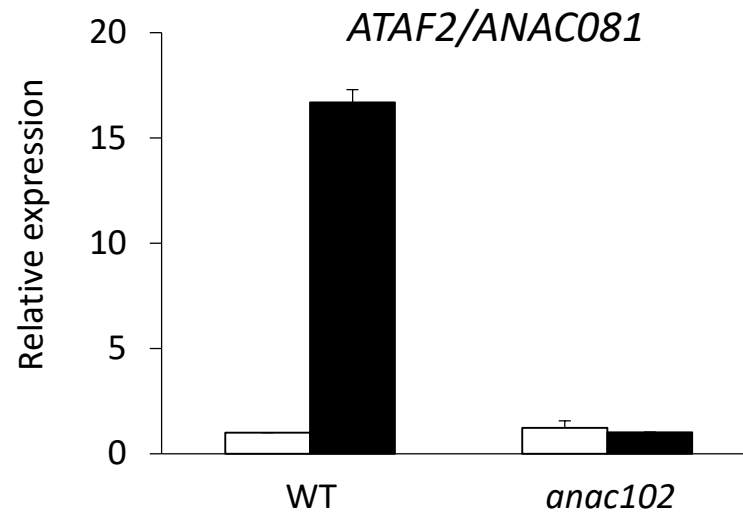
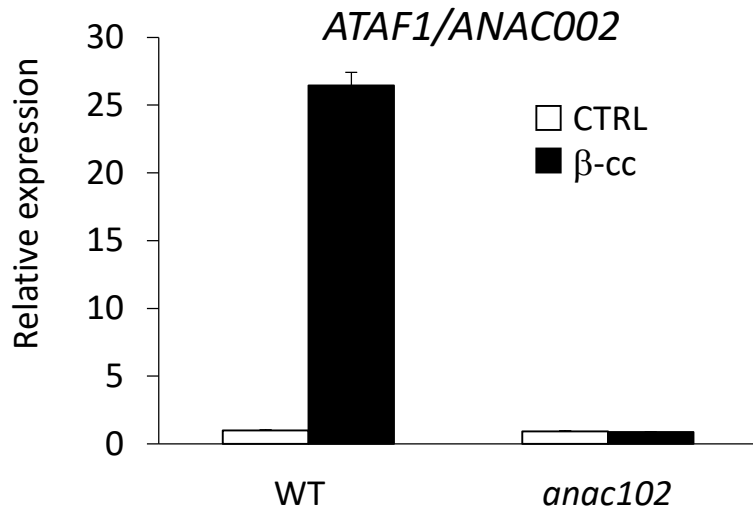


Figure 8: ANAC102 is upstream of ANAC002, ANAC032 and ANAC081

ANAC002, *ANAC032* and *ANAC081* expression levels (relative to wt control levels, CTRL WT, which were set to 1) in wt and *anac102* plants under control conditions or exposed to β -cc, measured by RT-qPCR. Every gene induced by β -cc in *anac102* plants showed a significant difference when tested against β -cc induction in the wt ($P < 0.01$). Error bars = + SD between the four technical replicates from pools of three plants per genotype per treatment.

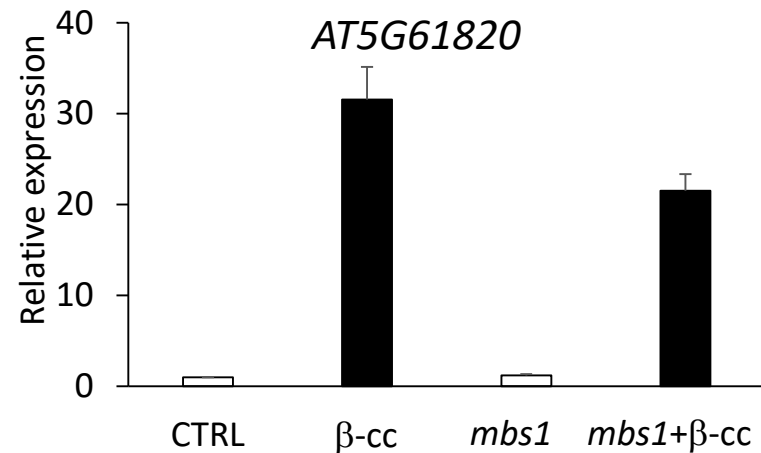
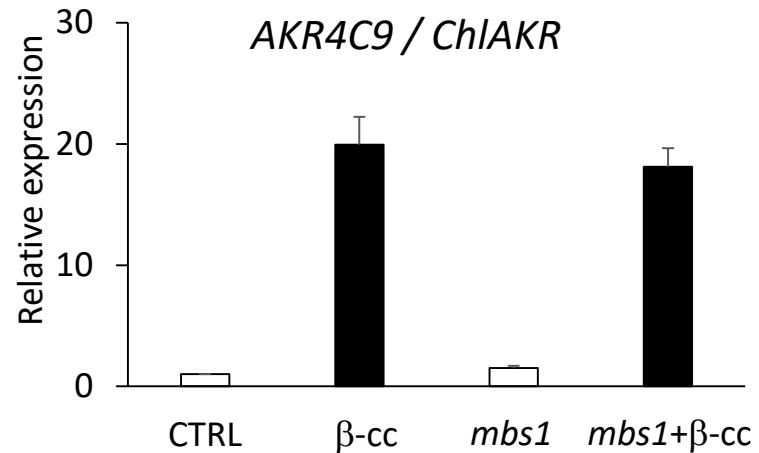
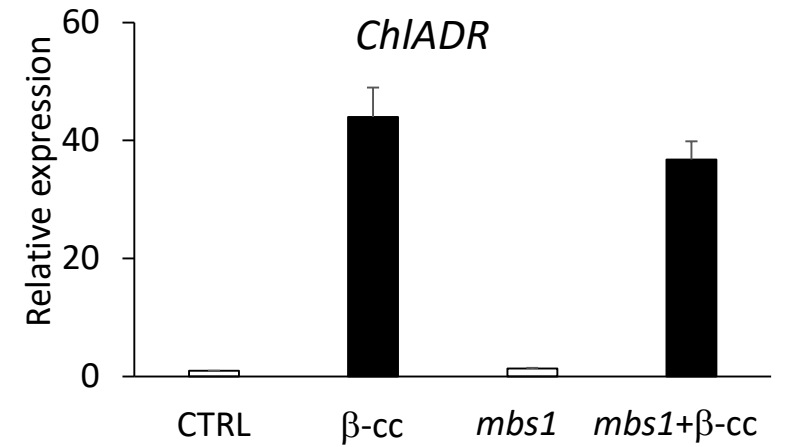
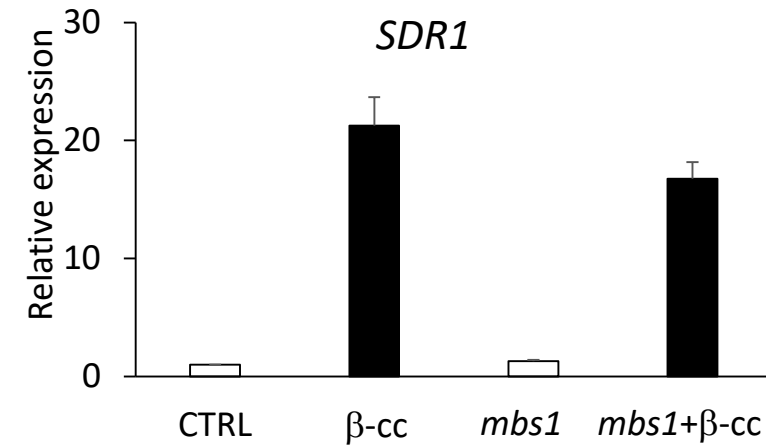
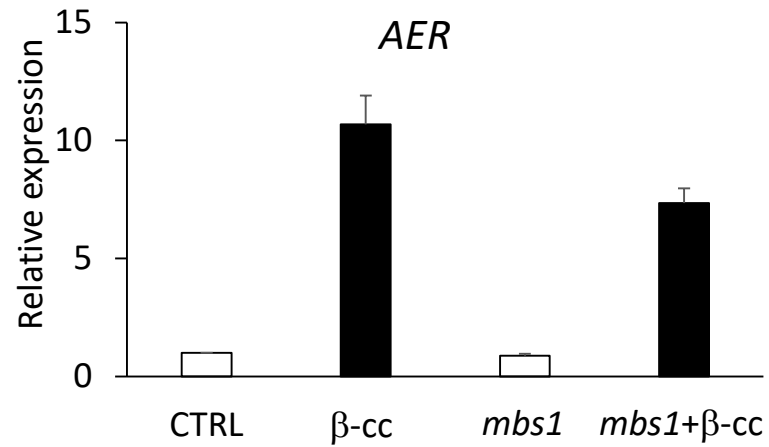
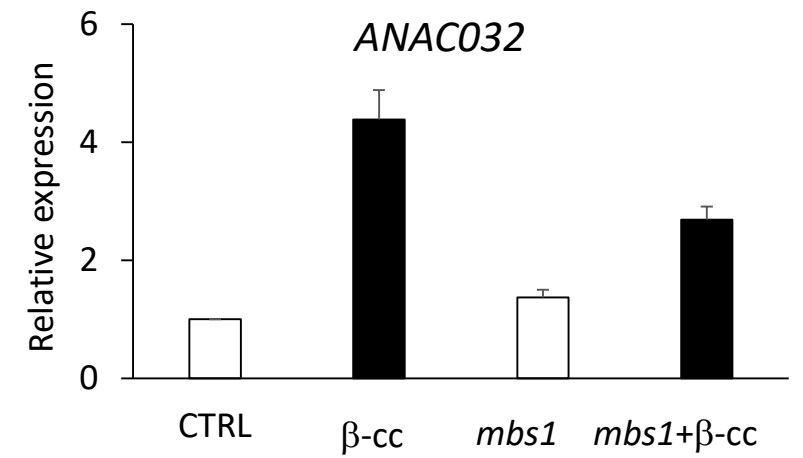
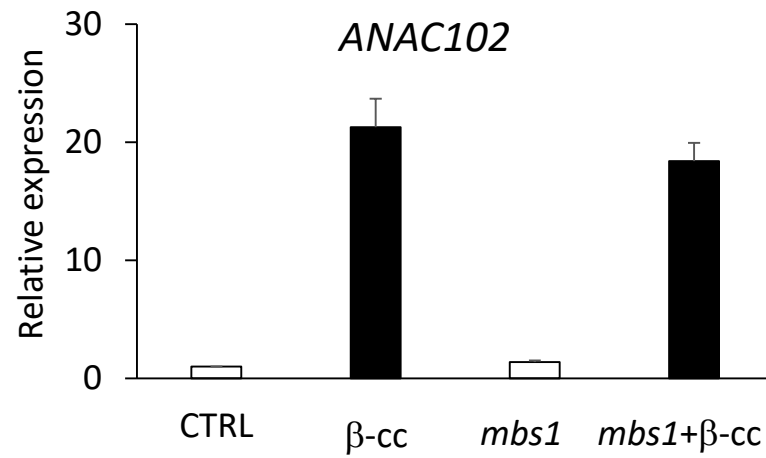
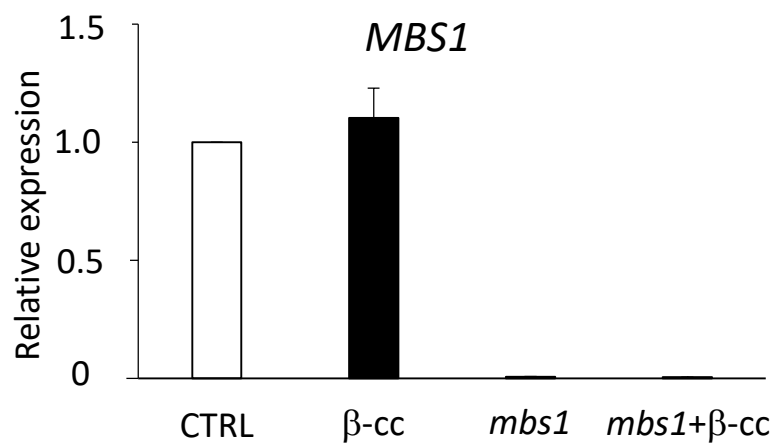


Figure 9: SCL14-dependent detoxification pathway is independent of MBS1

MBS1, *ANAC102*, *ANAC032*, *AER*, *SDR1*, *ChiADR*, *AKR4C9* and *AT5G61820* expression levels (relative to wt control levels, CTRL, which were set to 1) in wt and *mbs1* plants under control conditions or exposed to β-cc, measured by RT-qPCR. *MBS1* expression in the mutant is significantly lower than in wt ($P < 0,01$). *ANAC102*, *ANAC032*, *AER*, *SDR1*, *ChiADR*, *AKR4C9* and *AT5G61820* expression levels after β-cc treatment are significantly different from the relative control level in wt or *mbs1* mutant plants ($P > 0,01$). Error bars = + SD between the four technical replicates from pools of three plants per genotype per treatment. Two full experimental replicates

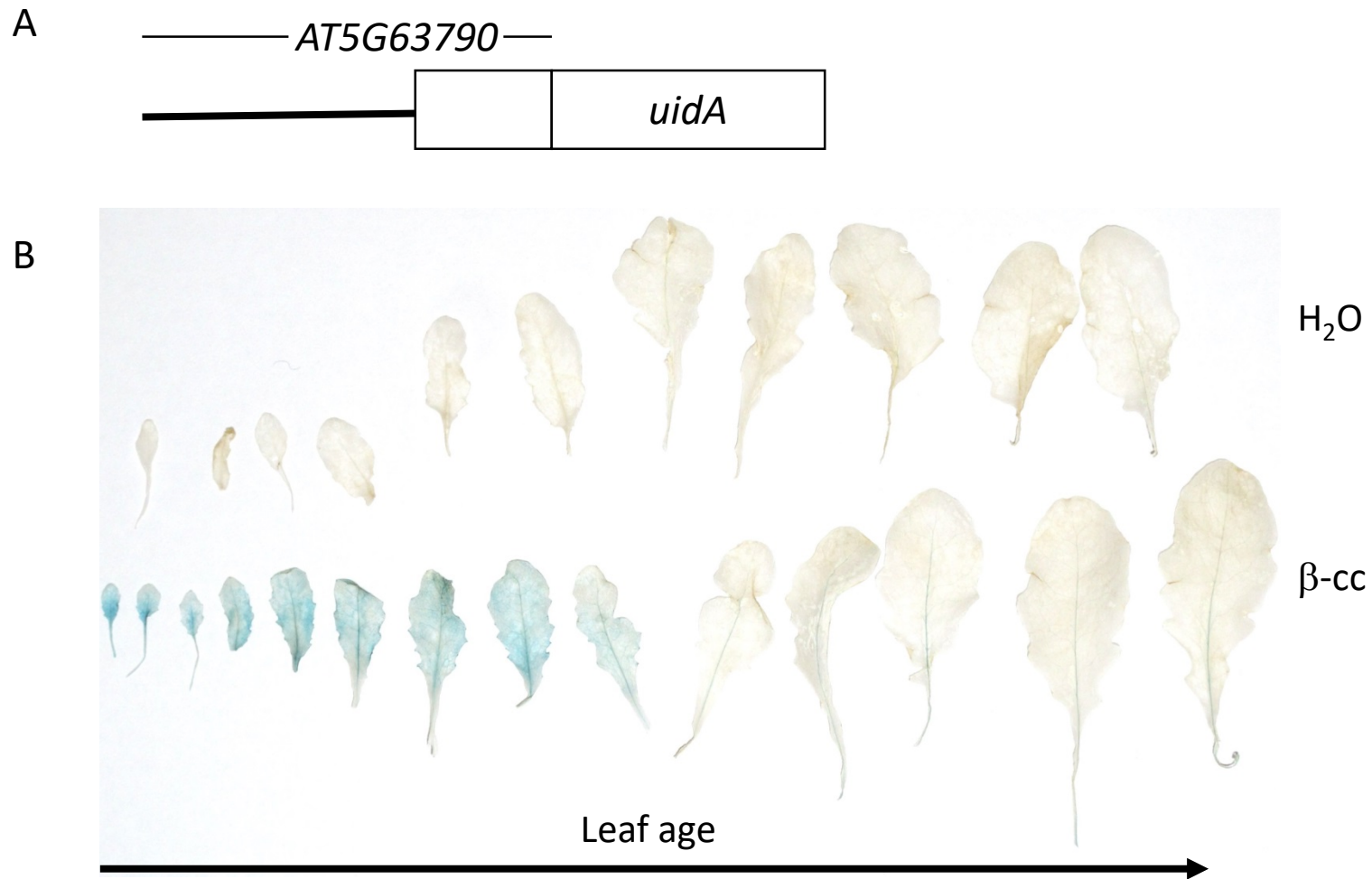


Figure 10: **ANAC102 is particularly induced in younger leaves**

(A) Schematization of the ANAC102 translational reporter. (B) Histochemical analyses of the translational reporter after 4h treatment with water (H₂O) or β -cc (β -cc) and overnight development of the staining. Two full experimental replicates.

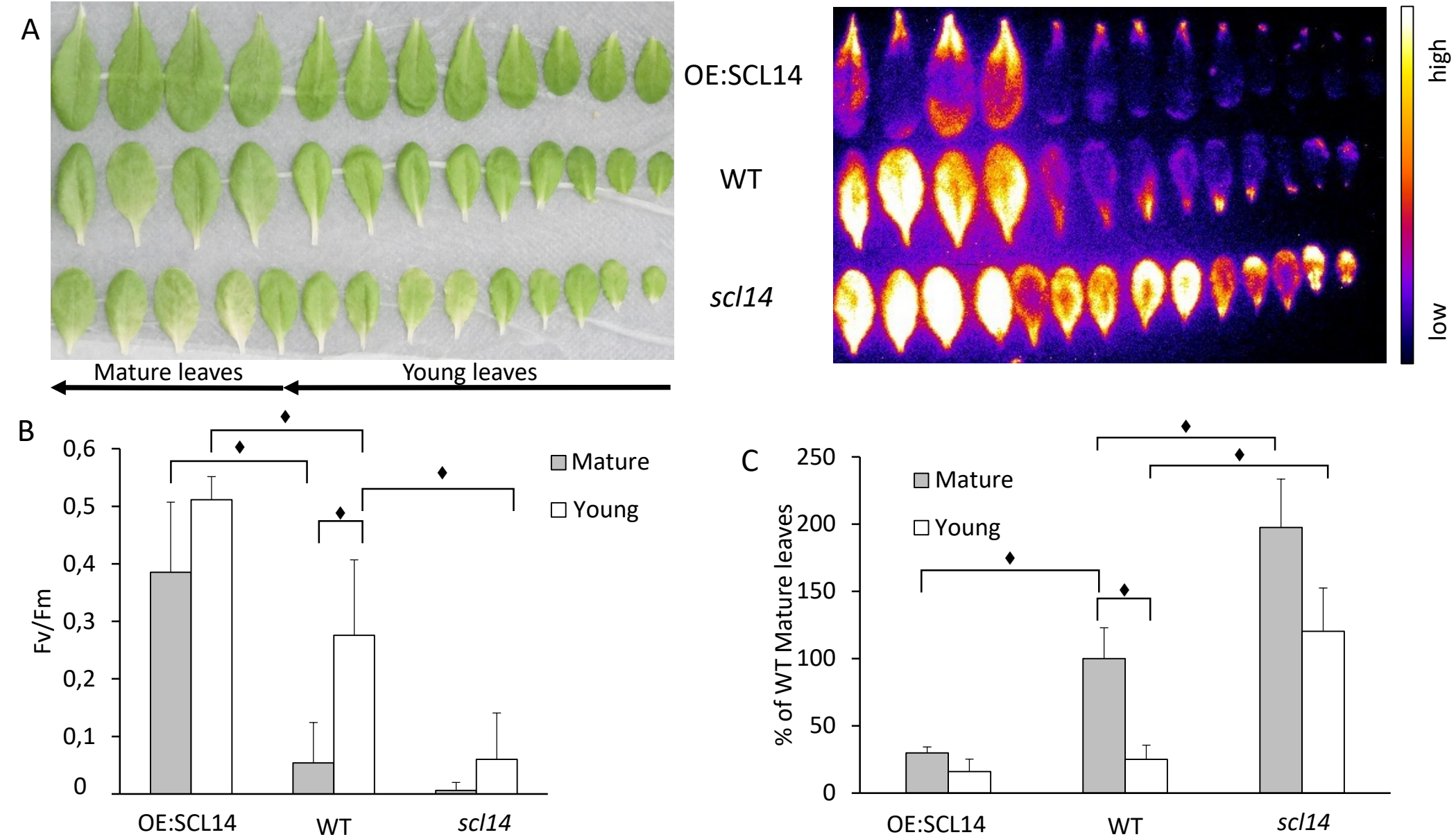


Figure 11: The resilience of young leaves to excessive light depends also on SCL14

(A) Leaf bleaching (on the left) and lipid peroxidation monitored by autoluminescence imaging (on the right) of wt, *scl14* and of OE:SCL14 detached leaves after high light stress. (B) Maximum quantum yield of PSII photochemistry determined by the Fv/Fm chlorophyll fluorescence ratio of wt, *scl14* and of OE:SCL14 mature and young detached leaves after high light stress. (C) HPLC-UV quantification of the HOTE normalized to wt mature leaves. Black diamonds indicate significant differences ($P < 0.05$). Error bars = + SD between the three biological replicates of pools of four mature leaves or ten young leaves. Two full experimental replicates.

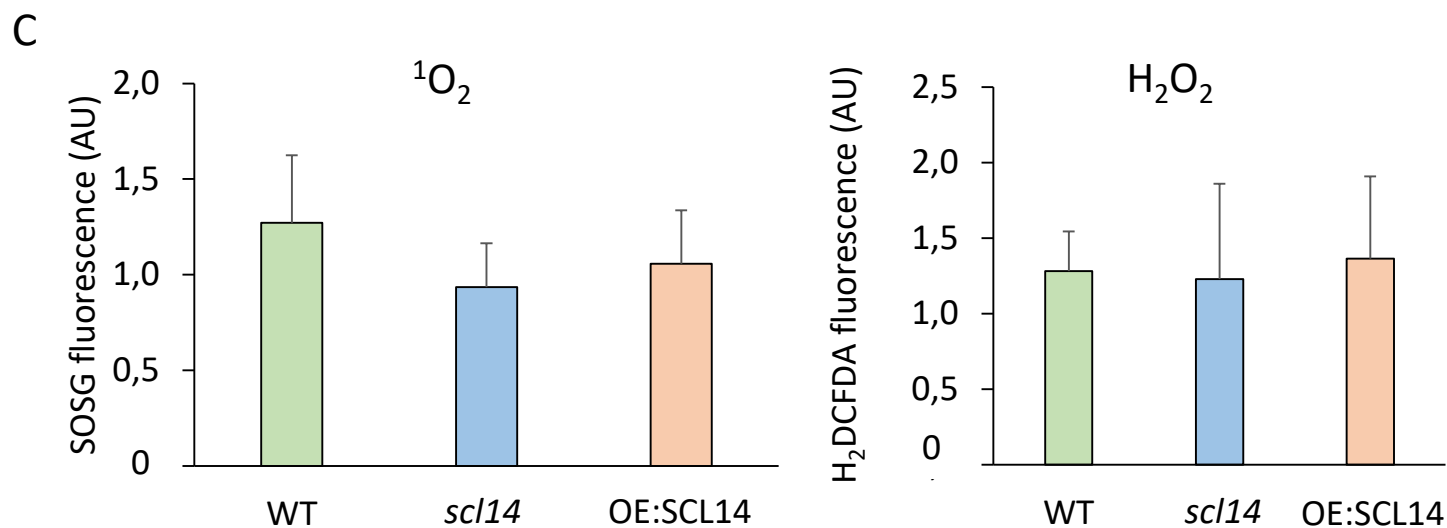
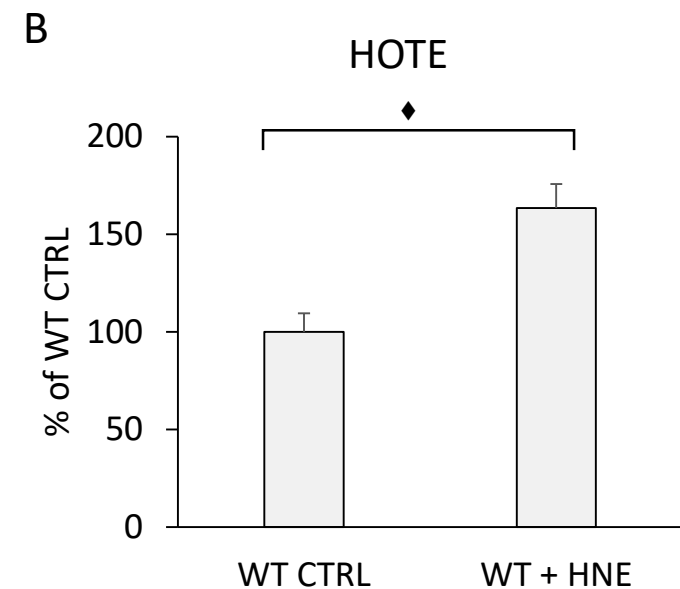
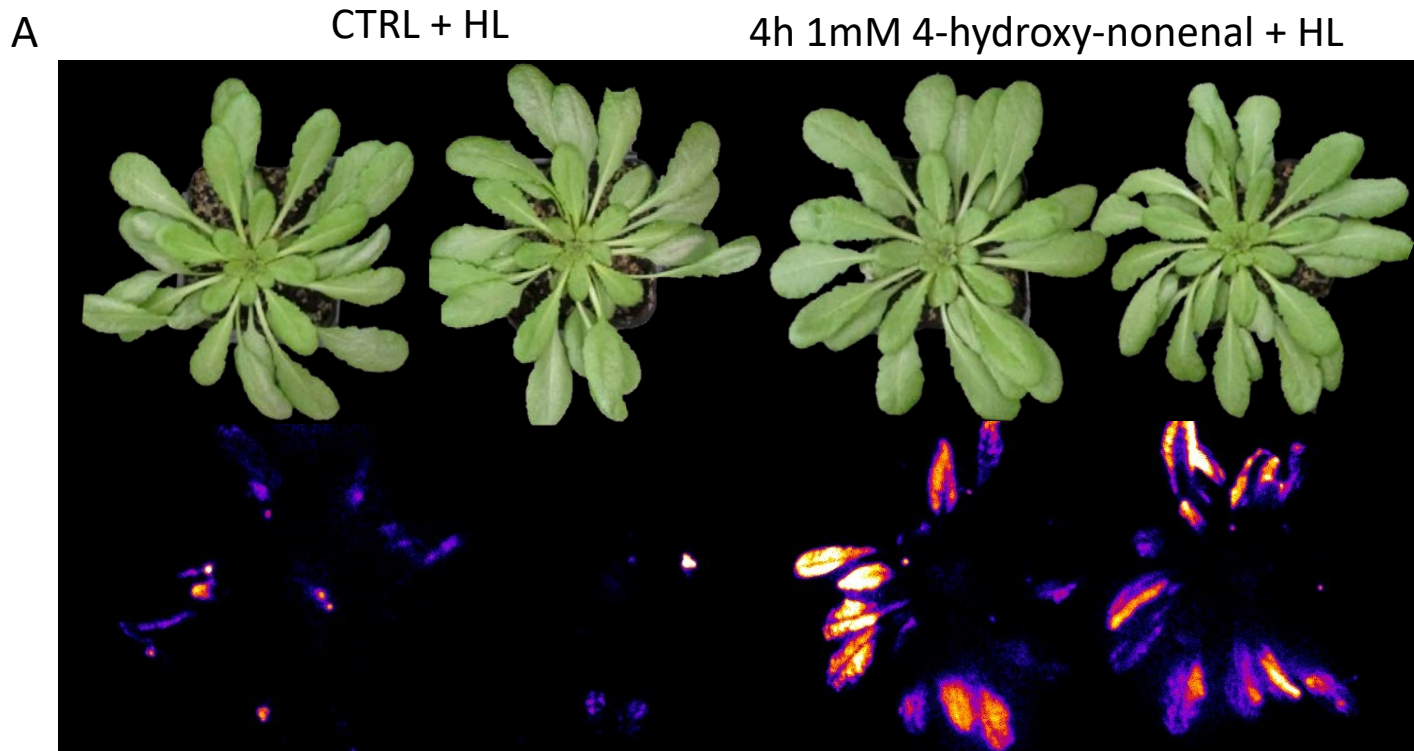


Figure 12: SCL14-dependent detoxification pathway acts on toxic RCS rather than on ROS accumulation

(A) Leaf bleaching (top panel) and lipid peroxidation, monitored by autoluminescence imaging (bottom panel), of WT plants pre-treated with 1 mM HNE or with water. The color palette shows signal intensity from low (dark blue) to high (white) values. (B) HPLC-UV quantification of the HOTE normalized to the wt control (CTRL). The black diamonds indicate significant differences with $P < 0.05$. Error bar = + SD between the four biological replicates from leaves of three plants per treatment. (C) SOSG or H₂DCFDA fluorescence in wt, *scl14* or OE:SCL14 plants tested measured after 4h of high light stress. Error bars = + SD between fluorescence deriving from five leaves per plant (Two plants per genotype per treatment).

EXCESSIVE LIGHT

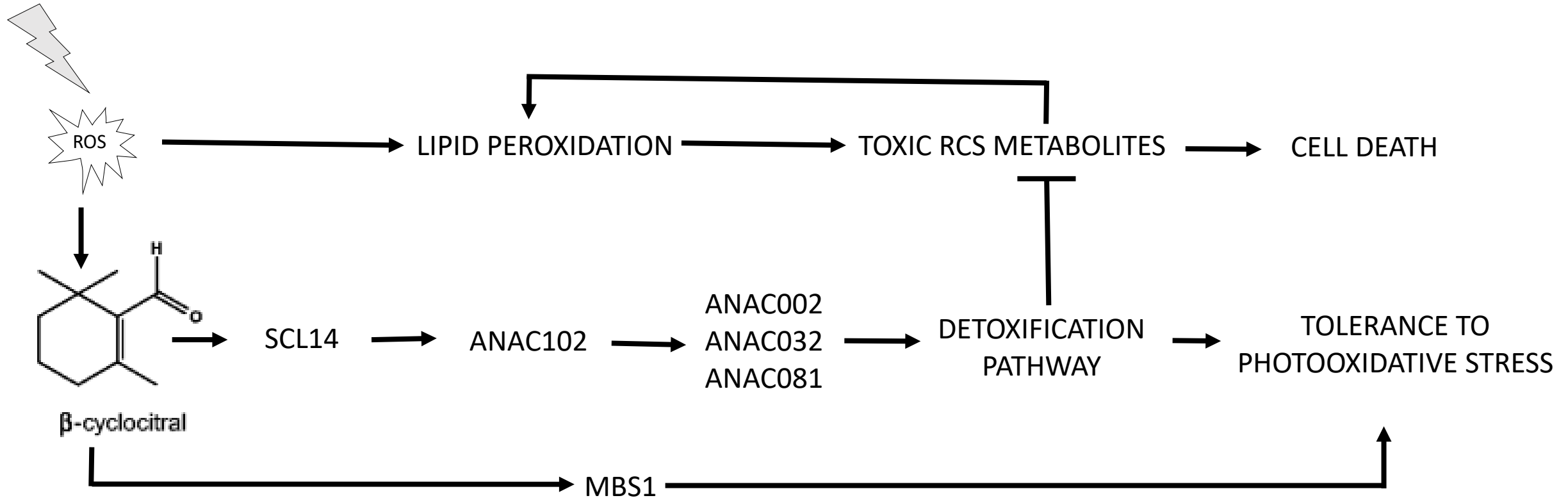


Figure 13. β -cyclocitral Mediates Resilience to Photooxidative Stress *via* the SCL14-dependent Xenobiotic Response

Photo-oxidation under excessive light stress generates toxic RCS metabolites and increases β -cc concentration. β -cc induces the expression of SCL14 leading to enhanced expression of ANAC102 and finally a strong activation of the xenobiotic detoxification response. In this response, ANAC102 is upstream of ANAC002, ANAC032 and ANAC081 expression, and consequently of the enzymes controlled by these transcription factors. Furthermore, the strong induction of the AER, AKRs, ALDHs and SDRs enzymes and of the glucosyl and glutathione transferases in the xenobiotic detoxification pathway assures the elimination of the RCS produced under stress conditions. Reducing RCS accumulation limits the positive feedback on lipid peroxidation and lead to tolerance rather than cell death.